Geologia Sudetica, 2009, 41: 25–42.

Palaeo- to Mesoproterozoic inheritance and Ediacaran anatexis recorded in gneisses at the NE margin of the Bohemian Massif: SHRIMP zircon data from the Nowolesie gneiss, Fore-Sudetic Block (SW Poland)

Krystyna Klimas[1], Ryszard Kryza[1] & Christopher Mark Fanning[2]

[1] *Institute of Geological Sciences, Wrocław University, ul. Cybulskiego 30, 50-205 Wrocław, Poland, e-mail: klim@ing.uni.wroc.pl*
[2] *Research School of Earth Sciences, The Australian National University, 0200 Canberra, Australia*

Key words: zircon, SHRIMP geochronology, anatexis, Strzelin Massif, Bohemian Massif, Fore-Sudetic Block, Variscides.

Abstract Recent geochronological studies, including sensitive high mass-resolution ion microprobe (SHRIMP) zircon dating, have helped to differentiate into specific age groups the various gneisses that occur within the basement units of the central-European Variscides. The Fore-Sudetic Block basement unit, for example, has been divided into two major gneiss groups of Neoproterozoic and Cambrian/Ordovician age, respectively. These two gneiss groups have been assigned to different tectonic units, themselves separated by a major tectonic boundary that is interpreted to be the northern continuation of the Moldanubian (Lugodanubian) Thrust. This thrust divides the main tectonostratigraphic units of the Bohemian Massif: the Moldanubian and Saxo-Thuringian units to the west, and the Moravo-Silesian unit to the east. This paper interprets new SHRIMP zircon data from the Nowolesie gneiss at Skalice (sample S6) and integrates the results with data from the Strzelin gneiss at Dębniki (sample S3), which is within the Strzelin Massif (E part of the Fore-Sudetic Block). Both the Nowolesie and Strzelin gneisses contain numerous inherited zircons within the age range of 1.5–2.0 Ga, indicating Meso- and Palaeoproterozoic sources for the zircons and suggesting that these zircons were recycled into younger units that subsequently underwent partial melting. The ages derived from samples S6 and S3, together with the absence of the Grenvillian ages (~1.3–0.9 Ga), suggest a West-African and/or Amazonian cratonic crust as the source for both the Nowolesie and Strzelin gneiss protoliths. The main zircon populations from both gneisses fall into two similar age groups: 602 ± 7 Ma and 587 ± 4 Ma for the Nowolesie gneiss; 600 ± 7 Ma and 568 ± 7 Ma for the Strzelin gneiss. These sets of Ediacaran (late Neoproterozoic) dates possibly reflect anatexis of the gneiss protoliths during the Cadomian orogeny.

Manuscript received 16 August 2009, accepted 30 November 2009

INTRODUCTION

REGIONAL GEOLOGICAL CONTEXT

The Fore-Sudetic Block (FSB), together with the neighbouring Sudetes to the west, forms the NE part of the Bohemian Massif. Crystalline rocks are poorly exposed in the E part of the FSB, whereas the lithostratigraphic variation is considerable (Fig. 1). For this reason, new petrological and geochronological investigations are needed to solve a range of geological problems of the NE margin of the Bohemian Massif and, on a wider scale, to decipher the pre-orogenic and orogenic evolution of the Central-European Variscides (e.g. Don, 1990; Matte *et al.*, 1990; Franke *et al.*, 1993; Cymerman *et al.*,1997; Aleksandrowski *et al.*, 2000; Finger *et al.*, 2000; Schulmann & Gayer, 2000; Franke & Żelaźniewicz, 2000; Timmermann *et al.*, 2000; Oberc-Dziedzic *et al.*, 2003b, 2005; Kryza *et al.*, 1996, 2004; Żelaźniewicz, 2003, 2005; Mazur *et al.*, 2006).

Despite many years of geological research, there remain debates concerning the genesis and ages of many FSB rock types, the definition of particular tectono-stratigraphic units and the location of some important tectonic boundaries in that part of the Bohemian Massif. For example, the Moldanubian Thrust zone, which is a pronounced tectonic boundary separating the internal zones of the Bohemian Massif from its external part represented by the Moravo-Silesian Zone (Suess, 1926; Kossmat, 1927; Oberc, 1957; Skácel, 1989), is better defined to the south but not

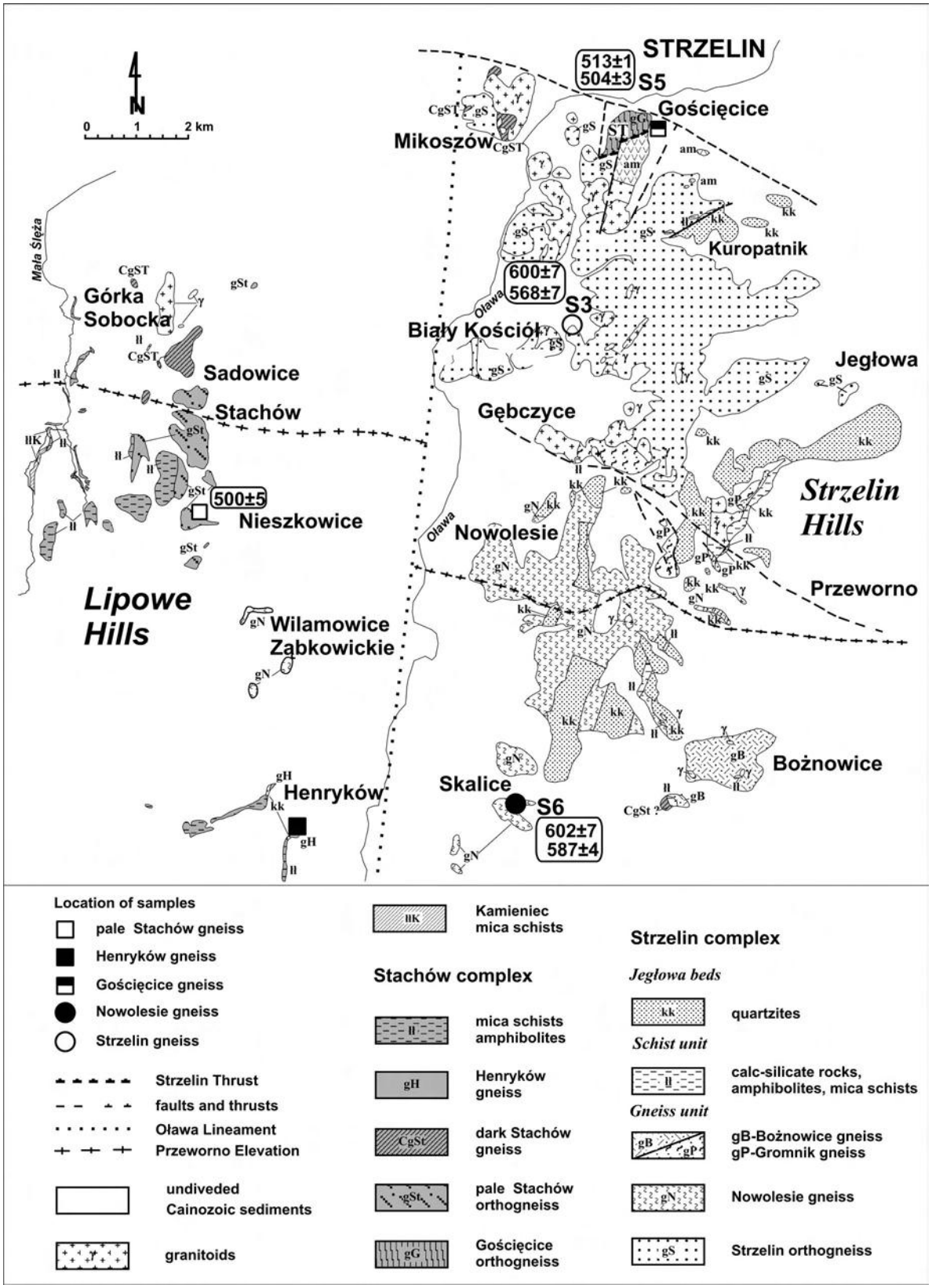

Fig. 1. Geological map of the Strzelin Hills and the Lipowe Hills (as modified by the authors after a compilation by Oberc-Dziedzic & Madej (2002) derived from maps in Oberc *et al.* (1988), Wójcik (1968), Wroński (1974), and Badura (1979)). The location of sample S6 and other samples discussed in this paper are indicated. The Strzelin Thrust (ST) is only locally recognized in the northern part of the area (south of Strzelin; Oberc-Dziedzic & Madej, 2002): its possible continuation along the Oława Lineament remains unresolved.

so evident to the north. In the mountainous area of the Sudetes, this thrust zone is taken as the tectonic boundary between the West and East Sudetes.

The West Sudetes comprise a mosaic of small geological units and are interpreted either as part of the W–E trending Saxo-Thuringian Zone (e.g. Franke *et al.*, 1993), a collage of several terranes (Matte *et al.*, 1990; Oliver *et al.*, 1993; Cymerman *et al.*, 1997; Cymerman & Piasecki, 2004; Aleksandrowski & Mazur, 2002; Żelaźniewicz, 2005), or a tectonic mosaic containing fragments of a Variscan accretionary prism (Baranowski *et al.*, 1990; Collins *et al.*, 2000). Nevertheless, despite the West Sudetes being lithostratigraphically diverse, a common feature is the presence of ~500 Ma orthogneisses.

Within the Moravo-Silesian Zone are the East Sudetes, which form a NNE–SSW trending belt that is separated from the West Sudetes by the Moldanubian Thrust zone (Oberc, 1957; Skácel, 1989). Schulmann and Gayer (2000) interpreted the Moravo-Silesian Zone as a continental accretionary wedge formed during the Variscan orogeny as a result of oblique collision between the Moldanubian and Lugian units and the Pan-African Bruno-Vistulian microcontinent (Dudek, 1980). The orthogneisses in the Bruno-Vistulian unit display late Neoproterozoic ages in the range of 546 +6/-8 to 684.5 ± 0.9 Ma (Oberc-Dziedzic *et al.*, 2005 and references therein).

Defining the Moldanubian Thrust zone further north, within the FSB, has been difficult due to poor exposure and uncertain ages. The thrust zone has, historically, been placed in four different positions: along the E edge of the Niemcza Shear Zone (Bederke, 1929); along the eastern boundary of the Strzelin Massif (Oberc, 1968); along the western boundary of the Strzelin Massif (Skácel, 1989); and within the Strzelin Massif itself (Cwojdziński & Żelaźniewicz, 1995). And at least one study (Cymerman, 1993a) did not recognise the existence of this tectonic boundary in the FSB. But recent study by Oberc-Dziedzic *et al.* (2003b, 2005) has delineated the thrust as within the Strzelin Massif, separating the Strzelin and Stachów structural units.

OUTLINE GEOLOGY AND TECTONOTHERMAL EVOLUTION OF THE STRZELIN MASSIF

In most publications on the FSB (Oberc, 1957, 1966, 1968, 1972, 1975, 1988; Bereś, 1969; Wójcik 1963, 1968, 1973; Cymerman, 1993b; Wojnar 1995; Oberc-Dziedzic, 1988, 1991, 1995, 1999; Oberc-Dziedzic & Szczepański, 1995; Oberc-Dziedzic *et al.*, 1996), the following three tectono-stratigraphic units in the E part of the FSB have been distinguished:

1. An older (Neoproterozoic–Lower Palaeozoic) metamorphic unit of gneisses, mica schists, amphibolites, calc-silicate rocks and marbles.

2. A younger metamorphic unit, the so-called Jegłowa beds, comprising lower and middle Devonian quartzites.

3. Variscan granitoids.

Based on the earlier studies cited above and on recent recommendations for clarifying the tectonic subdivisions of this part of the Fore-Sudetic Block (Żelaźniewicz & Aleksandrowski, 2008), two subordinate tectonic units can be distinguished in the northern part of the Strzelin Massif (the main tectonic basement unit in that part of the FSB): the Strzelin structural unit, and the Stachów structural unit. Their mutual contact is poorly exposed, though Oberc-Dziedzic and Madej (2002) consider them separated by the Strzelin Thrust, a feature only recognized in the northern part of the area (Fig. 1). Lithologically, two tectonostratigraphic units can be defined in that part of the Strzelin Massif: the Stachów complex and the Strzelin complex (Oberc-Dziedzic *et al.*, 2003a, b, 2005).

The Strzelin Massif is dominated by a variety of gneiss types: two-mica gneisses and granitic gneisses in the N, nodular sillimanite migmatitic gneisses in the S, and flaser-augen gneisses in a small outcrop at the NE margin (Oberc, 1966, 1968, 1972, 1975, 1988; Bereś, 1969; Wójcik, 1963, 1968, 1973; Wojnar, 1995). Oberc-Dziedzic (1995) named the gneisses of the Strzelin Massif after their most extensive outcrop localities: thus, the two-mica gneisses and the granitic gneisses are the Strzelin gneisses, the nodular sillimanite gneisses are the Nowolesie gneiss, and the flaser-augen gneisses are the Gościęcice gneiss. Based on drill-core samples, Oberc-Dziedzic (1995) also distinguished another significant variety, the dark migmatitic Stachów gneiss, and two transitional types: the pale, fine-grained Gromnik/Dobroszów gneiss, and the porphyroblastic sillimanite Bożnowice gneiss.

In the Lipowe Hills to the west (Fig. 1), mica schists are dominant (Badura, 1979; Wójcik, 1968, 1973; Wroński, 1974), a fact that was used as an argument to connect these schists with schists of the Niemcza Zone (Oberc, 1972). The most characteristic varieties of the subordinate gneisses in the Lipowe Hills are fine-grained dark gneisses and coarser-grained pale migmatitic gneisses, both of which are varieties of Stachów gneiss, and, in the S part of the area, mylonitic chlorite Henryków gneisses (Oberc-Dziedzic, 1995; Oberc-Dziedzic & Madej, 2002). In the Lipowe Hills, nodular-sillimanite migmatitic gneisses are also found and are similar to those in the Strzelin Hills (Oberc-Dziedzic, 1988). In drill-cores from the Strzelin Hills, Oberc-Dziedzic (1995) described rocks similar to the dark Stachów gneiss and, consequently, the western outcrop of the Lipowe Hills might be geologically related to the Strzelin Massif.

U–Pb SHRIMP zircon dating has helped to better define the two gneiss assemblages in the region: the Strzelin complex and the Stachów (Lipowe Hills) complex (Fig. 1; Oberc-Dziedzic *et al.*, 2003a, b, 2005; Klimas, 2008). In addition to its predominant gneiss content, the older Strzelin complex also contains mica schists, amphibolites, calc-silicate rocks and marbles. Furthermore, the relatively young gneiss and the mica schist of the Stachów complex have been thrust over the Strzelin complex along the Strzelin Thrust (Fig. 1; Oberc-Dziedzic *et al.*, 2003a, b, 2005).

Variscan tectono-metamorphic events are generally thought to have affected the rocks of the FSB (e.g. Cymerman, 1993b; Oberc-Dziedzic, 1995, 1999; Wojnar, 1995; Szczepański, 2001; Szczepański & Mazur, 2004). These

rocks experienced Devonian and early Carboniferous deformation and metamorphism that took place along different P–T paths in different units (Oberc-Dziedzic, 1999; Oberc-Dziedzic & Madej, 2002; Oberc-Dziedzic *et al.*, 2005). At least three metamorphic events are recorded in both the Neoproterozoic–Lower Palaeozoic gneiss and mica schist metamorphic unit and in the younger, Devonian, Jegłowa quartzites. The most pronounced metamorphic events, M_2 and M_3, were most intense in the southern part of the Strzelin Massif where the rocks experienced anatexis; in the northern part, however, the rocks only reached P–T conditions that occur at the boundary between greenschist and amphibolite facies (Oberc-Dziedzic, 1995, 1999; Oberc-Dziedzic *et al.*, 2005).

Important petrological information about the P–T path of the older Neoproterozoic–Lower Palaeozoic metamorphic complex has come from the calc-silicate rocks (Wojnar, 1955; Achramowicz *et al.*, 1996). Based partly on the earlier work of Oberc-Dziedzic (1988) and Wojnar (1995), Achramowicz *et al.* (1996) showed that this complex records a high temperature–medium pressue regional metamorphic event that corresponds to the upper part of the amphibolite facies, possibly transitional to the granulite facies. Achramowicz *et al.* (1996) also recognized a retrogressive, most likely anticlockwise, P–T path. The decrease in T, P, and probably also X_{CO2}, can be correlated with the early stages of uplift of the entire rock complex and in drastic changes of the pore fluids. Following that retrogressive phase, metamorphic reactions took place at increasing water activity.

The last Variscan tectonothermal event in the area of the FSB is the intrusion of the Variscan granitoids. These show a large scatter in their ages of between ~347 Ma and 290 Ma (Oberc-Dziedzic *et al.*, 1996; Oberc-Dziedzic & Pin, 2000; Pietranik & Waight, 2005; Turniak *et al.*, 2006), though these ages were obtained using different methods.

FORE-SUDETIC BLOCK: PREVIOUS ZIRCON GEOCHRONOLOGY

Zircon has been used in petrogenetical studies for more than half a century and specific morphologies have been used to infer specific petrogeneses (e.g. Pupin & Turco, 1972; Pupin, 1980, 1988; Majerowicz, 1975; Klimas-August, 1989; Guillot *et al.*, 2002; Klimas, 2008, and references therein). The U–Th–Pb and Pb–Pb geochronological methods that were developed during the 1950s, and subsequently refined, allow the age of zircon crystallization to be determined. These techniques can now be used to obtain separate ages for cores and overgrowths, not just bulk crystals (Davis *et al.*, 2003, and references therein). Complex internal zoning of zircons, invisible or barely visible using a polarizing microscope, may show up clearly using cathodoluminescence (CL) and back-scattered electron (BSE) imaging (e.g. Vavra, 1990, 1994; Benisek & Finger, 1993; Vavra *et al.*, 1996, 1999; Pidgeon, 1992; Pidgeon *et al.*, 2000; Rubatto & Gebauer, 2000; Rubatto *et al.*, 2001; Corfu *et al.*, 2003; Pankhurst *et al.*, 2006; Giacomini *et al.*, 2007).

Until relatively recently, there were only a few geochronological studies on the older crystalline basement rocks of the FSB. Oliver *et al.* (1993) reported a U–Pb evaporation multigrain zircon age of 504 ± 3 Ma from the Gościęcice gneiss (Fig. 1). This age was broadly confirmed later by Kröner and Mazur (2003) who reported 513 ± 1 Ma for the same rocks. Kröner and Mazur (2003) also determined the age of a migmatitic gneiss from Skalice in southern part of the Strzelin Massif and obtained a mean age of 1.020 ± 1 Ma for the main zircon population (six grains) and ages of between 1.1 and 1.8 Ma for the abundant zircon xenocrysts. Furthermore, they reported zircon ages of 501 ± 1 Ma (with a xenocryst core of 1.7 Ma) from granitic gneisses from Maciejowice and zircon ages of 380 ± 1 Ma (with a xenocryst core of 593 Ma) from granitic gneisses from Doboszowice, both south of the Strzelin Massif (beyond the map in Fig. 1). This data will be discussed in more detail below in light of the new SHRIMP results.

SCOPE AND AIMS OF THIS STUDY

In this paper we present new sensitive high mass-resolution ion microprobe (SHRIMP) zircon data for the Nowolesie gneiss at Skalice (Fig. 1), discuss the origin of this gneiss, compare this gneiss with other Precambrian gneisses in the Fore-Sudetic Block (FSB) and discuss some implications for the regional geology. The SHRIMP study reported here is part of a more extensive research project of using zircons to unravel the petrogenesis of the gneisses in the eastern part of the Fore-Sudetic Block (Klimas, 2008, and references therein). This paper specifically investigates the Nowolesie gneiss from Skalice because previous results yielded radically different ages from very similar gneisses from the Eastern FSB: 1.020 ± 1 Ma by Kröner & Mazur (2003); 600 ± 7 Ma by Oberc-Dziedzic *et al.* (2003b) and by Klimas (2008).

METHODS

Samples of Nowolesie gneiss were examined by thin section. On the basis of these observations, gneiss samples were selected for further zircon analyses. The selected samples were crushed in a jaw-crusher and sieved into several grain-size fractions. Zircon fractions were initially concentrated in a bowl of water, after which the magnetic fraction was separated, the remaining non-magnetic fraction being separated using sodium polytungstate. Finally, the zircons representing various types (based on classical "zirconology", see Klimas, 2008) were selected under the microscope for SHRIMP analysis.

Classical "zirconology" (including morphology, morphometry and typology) was performed using transmitted light under the polarizing microscope; observa-

tions were made on 100 zircon grains; only unbroken, euhedral and subhedral crystals were typologically classified (Pupin, 1980).

Cathodoluminescence (CL) images and SHRIMP-II measurements were carried out at the Australian National University in Canberra following procedures described in Williams (1998). The U/Pb ratios were determined using standard AS3 gabbro Duluth with $^{206}Pb/^{238}U = 0.1859$ and age of 1.099 Ma (Paces & Miller, 1993). Uncertainties at particular analyses and isotopic ratios are given at 1 sigma level. Terra and Wasserburg (1972) diagrams and mean weighted $^{206}Pb/^{238}U$ ages were calculated using the ISOPLOT/EX program (Ludwig, 1999)

PETROGRAPHY OF THE NOWOLESIE GNEISS

The petrography of the main gneiss varieties of the Strzelin and Lipowe Hills massifs has been compiled by Klimas (2008). The gneiss sample used herein is a portion of the sillimanite Nowolesie gneiss that was collected at Skalice and is here labelled as S6. It is a fine-grained, grey rock with a typical banded gneissic structure. The oriented texture is due to the parallel arrangement of biotite and flat lenses of fibrolite that are overgrown with muscovite and quartz. The gneiss is composed of quartz, plagioclase, K-feldspar, biotite, muscovite and sillimanite. Quartz is usually anhedral, locally in isometric grains. In places, a few aggregates of grains, flattened conformably with the foliation, can be seen. Plagioclase in the form of small plates is fresh and frequently twinned. Plagioclase compositions are within the range 8–13 % An (Wojnar, 1995).

In some samples of the Nowolesie gneiss, including sample S6, another variety of plagioclase is found: anhedral, often corroded grains, with cloudy and diffused twin lamellae along which sericite flakes have concentrated. These grains contain around 40 % An (Wojnar, 1995). K-feldspar is less abundant than plagioclase and usually forms large anhedral grains with common microcline twinning. Some of the grains enclose numerous sericite inclusions. Biotite forms elongated, imbricated flakes, parallel or oblique to the foliation; most often it is yellowish-brown, more rarely greenish in colour. Muscovite typically occurs as small irregular flakes and is, evidently, a secondary mineral formed after microcline, sillimanite and plagioclase (Wojnar, 1995). Sillimanite (fibrolite) is rather scarce. Most often it occurs in flattened aggregates together with muscovite and quartz that makes a specific nodular texture characteristic of these rocks. In some other gneisses, there are rare dispersed aggregates of fibrolite; in some gneiss varieties, there is also rare garnet and tourmaline. Zircon and small grains of opaques are common accessories (Fig. 2). Zircon forms isolated crystals in intersticies or occurs as inclusions in biotite and plagioclase.

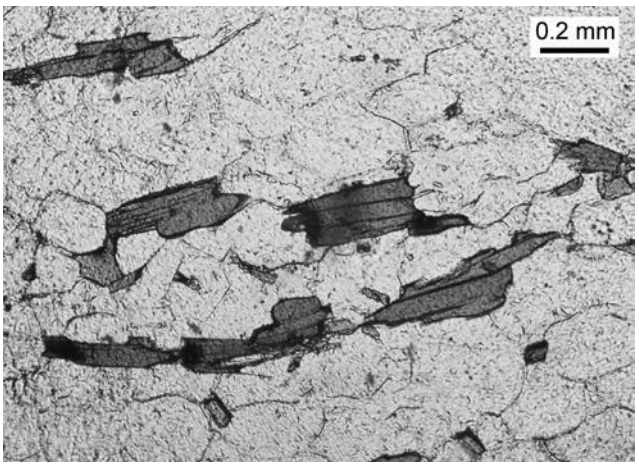

Fig. 2. Zircons in small biotite plates from the Nowolesie gneiss at Skalice (sample S6). The longer edge of the photo is 2 mm. Polarized light.

The Nowolesie gneiss mainly differs from the Strzelin gneisses that are widespread in the northern part of the Strzelin structural unit in the following ways: (a) there is an abundance of stromatitic and nebulitic textures in the Nowolesie gneiss, whereas porphyritic textures are common in the Strzelin gneisses; (b) the Nowolesie gneiss contains an abundance of sillimatite nodules; and (c) there is a widespread occurrence of pegmatite veins in the Nowolesie gneiss. A petrogenetically important feature is that the Nowolesie gneiss has low contents of zircon, and the Strzelin gneisses have less again. Zircon is significantly more abundant in the Gościęcice gneiss and in the pale varieties of Stachów gneiss. The observed zircon contents correspond to the bulk Zr concentrations in these rocks: 76 and 58 ppm in the Strzelin and Nowolesie gneiss, respectively; 221 and 223 ppm in the Gościęcice and Stachów gneiss, respectively (Oberc-Dziedzic *et al.*, 2005).

ZIRCON PETROGENESIS: THE NOWOLESIE GNEISS

A detailed petrogenetic study of zircons from selected gneisses of the Strzelin and Lipowe Hills massifs has been given by Klimas (2008).

In our sample S6 from the Nowolesie gneiss, 53 % of all zircons are euhedral and subhedral, 37 % subrounded, 1 % rounded, and 9 % irregular in habit. Among the euhedral and subhedral crystals, the most frequently observed are the types S_2, S_7 and S_8 of Pupin (1980) with a lesser number of S_1, S_{12}, S_{17}, S_5, G_1 (Fig. 3; Klimas, 2008). On the Pupin (1980) diagram, as modified by Guillot *et al.* (2002), these zircons fall in the field of anatectic granites (Klimas, 2008). However, on the modification of the Pupin diagram by Schermaier *et al.* (1992) these zircon types plot in the field of S-type granites. The zircons are

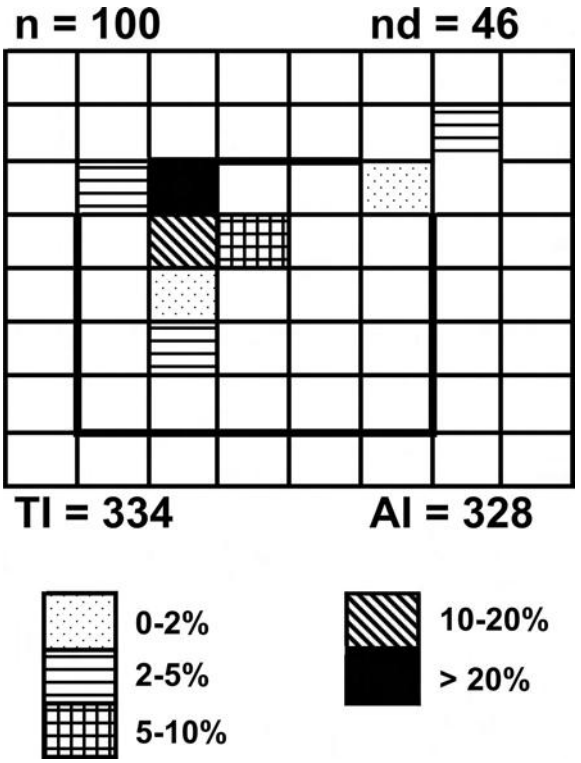

Fig. 3. Typology of zircons from the Nowolesie gneiss (sample S6) based on the scheme by Pupin (1980): n = number of grains investigated, nd = number of grains classified, TI = temperature index, AI = alkalinity index.

typical of the so called "cold" granites that crystallize below 837 °C and have a large amount of older zircon cores mantled by younger overgrowths (Klimas, 2008).

In CL images of zircons selected for SHRIMP analysis (Fig. 4), distinct cores mantled by younger overgrowths are visible in ~65 % of all grains. Thus, it was possible to distinguish (1) zircons with cores and overgrowths, and (2) zircons without cores.

ZIRCON CORES AND OVERGROWTHS

Zircon cores

The zircon cores in sample S6 from the Nowolesie gneiss are usually large and can form two-thirds to one-half of the whole crystal (Fig. 4: grains 2–4, 7, 10, 11, 19, 25–27, 29, 31, and 33–35); overgrowths, even if not very thick, display zonation (Fig. 4: 3, 4, 7, 13, 14, 25–29, 33, 34, 36). Smaller cores are rare and are often asymmetrically located within the crystal (Fig. 4: 5, 9, 10, 12, 13). However, most cores lie approximately near the center of the grain (Fig. 4: 2–4, 7, 25–29, 33, 34). The long axis of the cores and their crystallographic C axis are, in most cases, parallel to those of the overgrowth (Fig. 4: 2, 3, 7, 26, 29). Fairly common are cores displaying an extinction angle – the angle between the elongation axis and the C axis (Fig. 4: 4, 10–12, 25), a feature commonly interpreted as resulting from the transportation of detrital material (Klimas-August, 1989, and references therein). Overgrowths in such crystals imitate, at first, the form of the core, but they finally produce crystals with an elongation axis parallel to their C axis, suggestive of crystallization from a melt (Fig. 4: 4, 12, 25, 26).

The cores have various morphologies, the commonest being rounded and subrounded (Fig. 4: 2, 7, 26, 28). Others are subhedral and euhedral (Fig. 4: 3, 4, 29), but there are also irregular, corroded forms (Fig. 4: 27) and relatively common anhedral fragments of larger crystals (Fig. 4: 10–14). In some cores, the following Pupin (1980) types can be determined: G_1 (Fig. 4: 8), S_{17} (Fig. 4: 26), S_{24}, S_{25}, (Fig 4: 11–13). These types are characteristic of alkaline and calc-alkaline magmas. A few cores have preserved oscillatory zoning indicating their likely magmatic origin. Most of the cores, however, are homogeneous and CL bright, and such zircons, especially when having a low Th/U (0.1) ratio, are often interpreted as metamorphic zircons (e.g. Hacker *et al.*, 1998; Schaltegger *et al.*, 1999; Rubatto & Gebauer, 2000; Rubatto *et al.*, 2001). This interpretation does not, however, apply to similarly CL-homogeneous zircons from granulites that may have considerably higher Th/U ratios (Vavra *et al.*, 1996). Most of the cores in the sample described have the Th/U ratio above 0.1 (0.12–0.72; Fig. 5, Tab. 1). The CL homogeneity and brightness ("whitening") (Fig. 4: 19, 26) and, in some places, the relict convolute zonation (Fig. 4: 4) could have been caused by subsequent recrystallization, annealing or fluid activity (Vavra *et al.*, 1999).

One group of zircons posses CL-dark cores. These cores can be parallel-aggregates of a few crystals, or are corroded fragments that have been mantled by a thin overgrowth imitating the shape of the core. Sometimes these CL-dark cores are strongly corroded and irregularly shaped. These cores are composed of strongly metamict zircon and, thus, are more prone to corrosion than unaltered zircons.

Zircon overgrowths

The zircons that contain cores have euhedral or subhedral external habits, more rarely subrounded or anhedral. Because of the relatively large size of the cores, the thin overgrowths produce euhedral normal or long-prismatic crystals (Fig. 4: 3, 4, 26, 27, 29), though a few short-prismatic ones can also develop (Fig. 4: 7, 10, 12, 23, 25, 26, 31, 33). In CL, the overgrowths, when close to the core, display structures that are continuous with the core (Fig. 4: 2–4, 7, 25, 26), but further outwards these overgrowths usually become, and continue to be, euhedral (Fig. 4: 14). However, this is not the type of oscillatory zonation that is found in typical magmatic zircons (e.g. Pidgeon *et al.*, 1998; Hoskin, 2000; Corfu *et al.*, 2003), where particular zones alternate between CL-bright and CL-dark layers. Here, in sample S6, this zonation is not very regular. It is usually distinct within the pyramids, especially in crystals containing large cores (Fig. 4: 3, 4, 25, 29, 34, 36). In such crystals the growth is limited along the prism and it continues mainly within the pyramids. The internal form of the overgrowth is dominated by pyramid {101} with subordinate steep pyramid {211}, and the final crystallization prefers the growth of {211} to that of {101} (Fig. 4: 3, 4, 7). If the core endings are originally steep, the

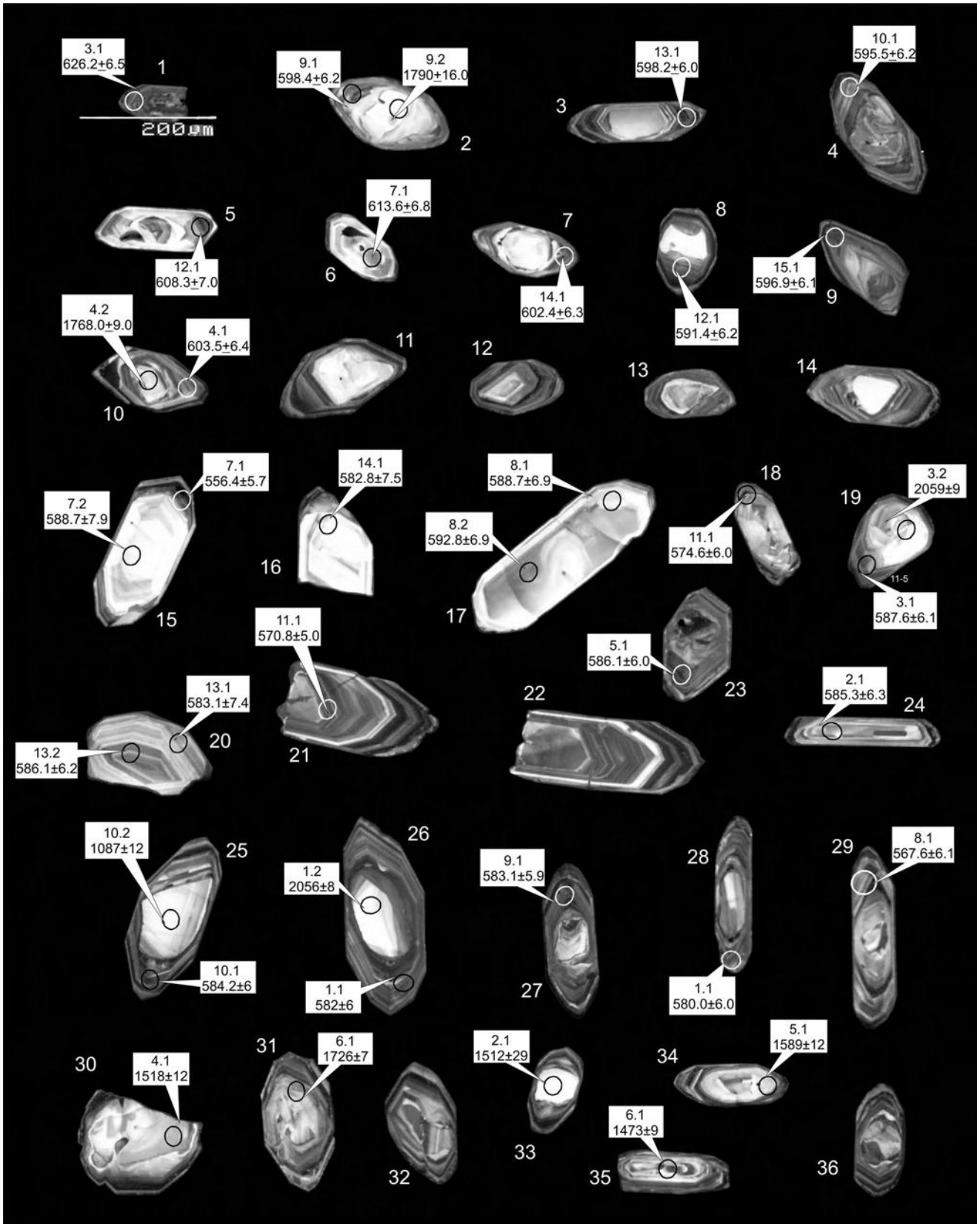

Fig. 4. Cathodoluminescence images of zircons from the Nowolesie gneiss at Skalice (sample S6). Zircon grains numbered 1 to 36 are referred to in the text. SHRIMP analytical spots are indicated by ellipses ~25 μm large; Pb/U ages for Neoproterozoic and younger zircons, and Pb/Pb ages for older Precambrian zircons (1σ errors) are given in labels.

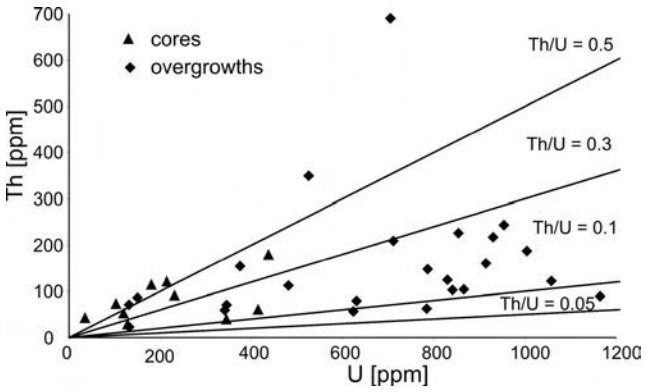

Fig. 5. Plot of Th/U ratio in zircons from the Strzelin and Nowolesie gneiss within the Strzelin Massif.

new overgrowth from the very beginning continues with {211} predominating over {101} (Fig. 4: 12, 13, 25, 26, 28, 29).

This kind of growth results in a predominance of crystals with the steep pyramid located in the upper left and bottom left parts of the Pupin (1980) diagram (Fig.3), with either of the prisms {110} or {100} being dominant. As a consequence, it is difficult to define a clear crystallization trend for the zircons from sample S6 because the morphologies converge on three trends of zircon crystallization that, in the diagram, define early and advanced crystallization phases for calc-alkaline and peralkaline magmas.

Sporadically, multifaceted prismless forms are observed on the one crystal where one end is relatively broad and nearly isometric, while the other end is relatively narrow (Fig. 4: 9, 11, 12, 19). The space between the core and the youngest zoned part of the overgrowth is locally filled by sector-zoned zircon (Fig. 4: 9, 25). These zircons are particularly common in the <0.12 mm fraction and are normally excluded from this study due to the difficult separation of such small grains. But when observed in transmitted light in heavy mineral separates, they tend to be classified as subrounded and rounded because their multifaceted nature is only visible in CL images. Similar zircons have been reported from granulite-facies "leptynites" in the Vosges (Schaltegger *et al.*, 1999), as well as in the granulites and gneisses of the Ivrea Zone in the Southern Alps (Vavra *et al.*, 1996; Vavra *et al.*, 1999).

At the boundary between core and overgrowth in a few crystals is a distinct layer, very dark or nearly black in CL image (Fig. 4: 4, 12, 25, 26, 28, 29, 31, 33, 34). A similar zone can also be found along the margin of the euhedral overgrowth (Fig. 4: 4, 10, 25, 27, 30, 36). The next layer, brighter in CL, is often incomplete and seems to have been corroded by residual melt or fluids (Fig. 4: 2, 3, 14, 28, 31, 32, 35, 36). The CL-dark layers usually indicate high trace element and rare-earth element contents, in particular uranium and yttrium, but may also indicate intense metamictization. The causes of CL-dark layers can be distinguished, however, using BSE images on the dark layers: intense metamictization causes the CL-dark regions to remain dark using BSE images; but CL-dark regions rich in heavy elements are bright in BSE (e.g. Kempe *et al.*, 2000; Silva *et al.*, 2000).

The presence of the internal and external CL-dark layers, usually rich in U, Th and other heavy and rare-earth elements, probably results from diffusion of these elements in a closed system (Pidgeon *et al.*, 1998). In an open system, the marginal layer usually disappears due to the removal of these elements out of the system. In the early phases of this process, external layers become wider and "whitened" but their euhedral nature is preserved. During the more advanced phase of the process of recrystallization and fluid interaction the CL zonation becomes disturbed, the "whitened" layers become lobate and "ghost zoning" is poorly preserved (Fig. 4: 16, 18).

There is one more important feature of the zircons with cores: they represent two populations of different ages. The age relationships and differences in morphology and morphometry will be described below.

ZIRCONS WITHOUT CORES

The zircon crystals without cores are subordinate within the whole zircon population. They are, nevertheless, very diverse in their morphology, morphometry, typology and internal structure (Figs. 2 & 4). Two groups of two different ages can be distinguished (see below).

Group A (older zircons) (Fig. 4: 1, 5, 6, 8) occur mainly in the finer grain-size fraction, .12 mm. Most often they are short-prismatic, CL-bright, with weakly preserved "ghost" zonation (Fig. 4: 6) and with a Th/U ratio of 0.41. More rarely, they are football-shaped, multifaceted and CL-bright, with almost no traces of zonation (Fig. 4: 8), with Th/U ratio of 0.09.

Group B (younger zircons) are larger crystals, up to 0.25 mm (Fig. 4: 15). Most are "whitened" (Fig. 4: 15–19), with oscillatory zonation easily visible (Fig. 4: 20, 24) or, at times, poorly preserved as "ghost" zonation (Fig. 4: 15, 17).

Within the euhedral zircon crystals without cores, very long-prismatic, "needle-like" forms are found, often with an elongated inclusion along the central section (e.g. Fig. 4: 24). These long-prismatic crystals are interpreted as the products of rapid crystallization from a melt with high Zr oversaturation (Klimas & Szczepański, 2005, and references therein).

Another group of zircons comprises euhedral crystals, but also fragments of larger crystals, both of which show strong oscillatory zonation (Fig. 4: 21, 22). Based on the zonation patterns, initial crystallization was dominated by the formation of the "flat" pyramid {101}, often asymmetrically, and was later joined by the steep pyramid {211}, which subsequently came to dominate the morphology. After crystallization, both types of pyramid underwent corrosion, as observed from external CL-bright layers. The broken surfaces of crystals are rough and only slightly corroded.

The CL images show the presence of a large amount of broken crystals in both the large and small size fractions; these represent either one-third, one half or three-quarters of unbroken euhedral crystals (Fig. 4: 1, 16, 21, 22). Most display clear mechanical defects on their broken

surfaces and most are either fragments of larger euhedral crystals that display well-preserved, typical, magmatic oscillatory zoning (Fig. 4: 21, 22), or are fragments of large "whitened" crystals (Fig. 4: 16) with high Th/U ratio of 0.57, or are "whitened" euhedral grains with notched edges (Fig. 4: 17).

In a few grains such broken surfaces have been mechanically smoothened, as might happen during detrital-grain or tectonic transportation. These particular smoothened surfaces are not, however, an effect of magmatic corrosion.

SHRIMP DATA ON ZIRCONS FROM THE NOWOLESIE GNEISS

SHRIMP analyses, from zircons in sample S6 of the Nowolesie gneiss, were performed on 10 points located in zircon cores and on 27 points in overgrowths and in homogeneous core-absent crystals (Table 1; Figs. 4, 5, 6, 7 & 8). All these measurements and subsequent recalculations were performed for both grain-size fractions separately (0.16–0.12 mm and 0.12–0.06 mm).

Zircon cores

There was a wide scatter of ages from the zircon cores. Concordant core ages included Palaeoproterozoic $^{207}Pb/^{206}Pb$ ages (2.056 ± 8 Ma–1.726 ± 7 Ma) and Mesoproterozoic ages (1.589 ± 12 Ma–1.473 ± 9 Ma) (Table 1; Fig. 6). Discordant core ages (Fig. 6), such as from points 3.2 and 10.2 from the coarser fraction and from point 9.2 from the finer fraction, probably reflect Pb loss. Point 3.2 is from the center of a crystal without any distinct core, faint "ghost" zonation and CL-"whitening", and produced a $^{207}Pb/^{206}Pb$ age of 2.059 ± 9 Ma (Fig. 4: 19) and Th/U = 0.57. This may indicate annealing, recrystallization or fluid activity. Point 10.2, also from the coarser fraction, was taken from within a CL-bright core that had signs of mechanical damage and gave an age of 1.007 ± 12 Ma with high Th/U = 0.72. This was probably due to sedimentary reworking (Fig. 4: 25). Point 9.2, from the finer fraction and taken in the core of a zircon displaying symptoms of recrystallization and external corrosion, had an age of 1.790 ± 16 Ma and Th/U = 0.23 (Fig. 4: 2).

Comparing the U and Th concentrations and the Th/U ratios in the zircon cores with those in the overgrowths and younger crystals without cores reveals considerably lower U and Th concentrations and higher Th/U ratios in the latter (Table 1, Fig. 5). There is also a sharp difference in $^{207}Pb/^{206}Pb$ and $^{206}Pb/^{238}U$ ages in the cores of zircons from different grain-size fractions. The ages of cores in zircons from the coarser fraction are, in general, older even after excluding the points with relatively significant discordance (Table 1).

Overgrowths and zircons without cores

No significant differences in U and Th concentrations and in Th/U ratios can be detected in the overgrowths and younger zircons of both grain-size fractions (Table 1). However, two age generations can be distinguished that exactly follow grain size. Zircons from the finer fraction mostly have overgrowths and core-absent crystals and are of an older generation with a $^{206}Pb/^{238}U$ probability density age of 602 ± 7 Ma. Zircons from the coarser grain fraction are younger with a $^{206}Pb/^{238}U$ probability density age of 587 ± 4 Ma (Fig. 9, Table 1).

There is a negative relationship between the weighted mean $^{206}Pb/^{238}U$ ages of both the overgrowths and the

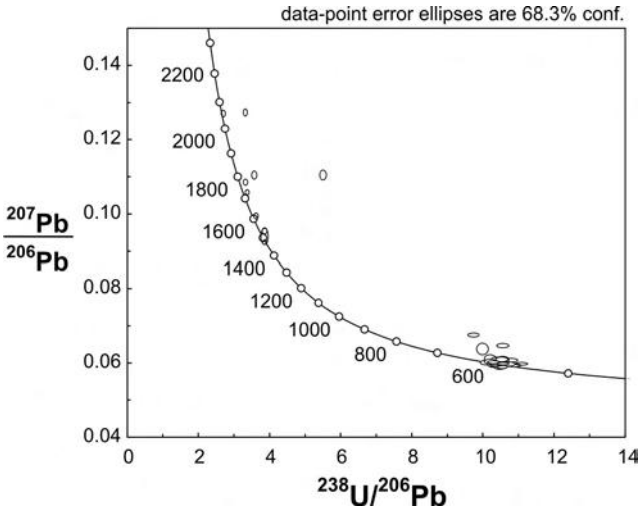

Fig. 6. Terra and Wasserburg (1972) concordia plot of zircons from the Nowolesie gneiss at Skalice (sample S6). The plot shows the total Pb/Pb ratios vs. the calibrated U/Pb ratios, uncorrected for common Pb. Analyses are plotted as 1σ error ellipses.

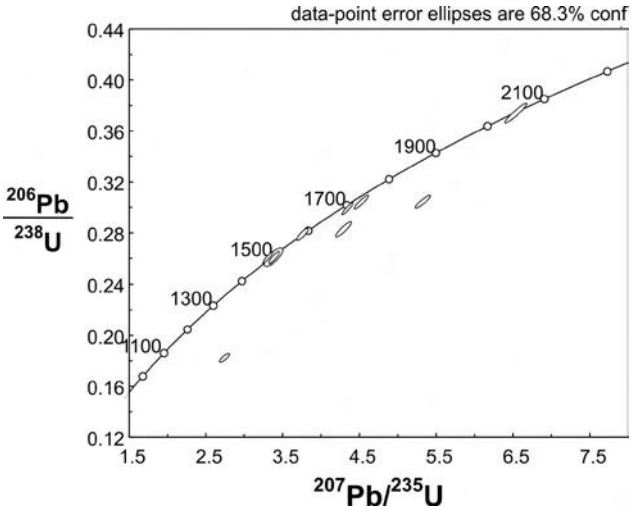

Fig. 7. A Wetherill plot (using the Isoplot/Ex program by Ludwig, 1999) for Proterozoic zircons from the Nowolesie gneiss at Skalice (sample S6). Plot shows the Pb/U ratios vs. the Pb/U ratios. Analyses are plotted as 1σ error ellipses.

SHRIMP UPb data on zircons from the Nowolesie gneiss at Skalice (sample S6) **Table 1**

Grain. spot	U (ppm)	Th (ppm)	Th/U	Pb* (ppm)	$^{204}Pb/^{206}Pb$	f_{206} %	Total Ratios $^{238}U/^{206}PB$	±	$^{207}Pb/^{206}Pb$	±	Radiogenic Ratios $^{206}Pb/^{238}U$	±	$^{207}Pb/^{235}U$	±	$^{207}Pb/^{206}Pb$	±	r	Age (Ma) $^{206}Pb/^{238}U$	±	$^{207}Pb/^{206}Pb$	±	% Disc
0.12 to 0.16																						
1.1	830	125	0.15	67	0.000060	0.15	10.567	0.112	0.0607	0.0004	0.0945	0.0010						582	6			
1.2	119	53	0.45	38	0.000006	0.01	2.676	0.037	0.1270	0.0006	0.3736	0.0051	6.537	0.094	0.1269	0.0006	0.949	2046	24	2056	8	0
2.1	525	349	0.67	43	0.000031	<0.01	10.527	0.116	0.0590	0.0005	0.0950	0.0011						585.3	6.3			
3.1	784	63	0.08	64	0.000029	0.03	10.475	0.112	0.0598	0.0005	0.0954	0.0010						587.6	6.1			
3.2	214	122	0.57	56	0.000002	0.00	3.289	0.037	0.1272	0.0006	0.3040	0.0034	5.332	0.065	0.1272	0.0006	0.913	1711	17	2059	9	17
4.1	232	92	0.40	52	0.000056	0.09	3.836	0.044	0.0953	0.0006	0.2604	0.0030	3.394	0.045	0.0945	0.0006	0.878	1492	15	1518	12	2
5.1	1004	187	0.19	82	0.000052	0.01	10.505	0.111	0.0596	0.0003	0.0952	0.0010						586	6			
6.1	414	61	0.15	106	0.000002	<0.01	3.348	0.036	0.1057	0.0004	0.2986	0.0032	4.351	0.050	0.1057	0.0004	0.940	1685	16	1726	7	2
7.1	1164	89	0.08	90	-	0.11	11.081	0.116	0.0596	0.0003	0.0902	0.0010						556	6			
7.2	131	71	0.54	11	-	0.05	10.452	0.143	0.0600	0.0007	0.0956	0.0013						589	8			
8.1	131	23	0.17	11	0.000118	<0.01	10.463	0.125	0.0592	0.0007	0.0956	0.0012						589	7			
8.2	342	59	0.17	28	0.000096	0.09	10.374	0.123	0.0604	0.0006	0.0963	0.0012						593	7			
9.1	1425	314	0.22	116	0.000003	0.03	10.559	0.110	0.0597	0.0002	0.0947	0.0010						583	6			
10.1	865	104	0.12	71	0.000029	0.16	10.525	0.112	0.0608	0.0004	0.0949	0.0010						584	6			
10.2	103	74	0.72	25	-	<0.01	3.541	0.050	0.1103	0.0007	0.2825	0.0040	4.302	0.067	0.1105	0.0007	0.906	1604	20	1807	12	11
11.1	711	209	0.29	57	0.000023	0.18	10.781	0.114	0.0606	0.0003	0.0926	0.0010						571	6			
12.1	623	56	0.09	51	0.000040	<0.01	10.408	0.113	0.0597	0.0004	0.0961	0.0011						591	6			
13.1	346	70	0.20	28	0.000100	0.04	10.559	0.138	0.0598	0.0006	0.0947	0.0013						583	7			
13.2	481	113	0.23	39	0.000040	<0.01	10.512	0.114	0.0591	0.0005	0.0952	0.0010						586	6			
14.1	150	86	0.57	12	0.000105	0.10	10.558	0.139	0.0603	0.0009	0.0946	0.0013						583	8			
0.06 to 0.12																						
1.1	954	244	0.26	78	0.000451	0.63	10.556	0.112	0.0645	0.0004	0.0941	0.0010						580	6			
2.1	35	43	1.24	8	-	<0.01	3.835	0.068	0.0938	0.0014	0.2609	0.0047	3.388	0.080	0.0942	0.0014	0.758	1494	24	1512	29	1
3.1	914	160	0.18	81	0.000010	0.82	9.721	0.103	0.0674	0.0004	0.1020	0.0011						626	6			
4.1	631	79	0.13	53	0.000059	0.03	10.186	0.111	0.0602	0.0004	0.0981	0.0011						604	6			
4.2	180	115	0.64	47	0.000022	0.03	3.291	0.040	0.1084	0.0005	0.3037	0.0037	4.528	0.060	0.1081	0.0006	0.922	1710	18	1768	9	3
5.1	345	40	0.12	83	0.000085	0.14	3.587	0.040	0.0993	0.0005	0.2784	0.0031	3.767	0.048	0.0981	0.0006	0.866	1583	16	1589	12	0
6.1	437	180	0.41	98	-	<0.01	3.842	0.042	0.0922	0.0004	0.2603	0.0028	3.313	0.039	0.0923	0.0004	0.923	1492	14	1473	9	-1
7.1	375	154	0.41	32	0.000087	0.41	9.974	0.113	0.0636	0.0011	0.0999	0.0012						614	7			
8.1	1058	122	0.12	84	-	0.03	10.861	0.120	0.0592	0.0003	0.0920	0.0010						568	6			
9.1	786	148	0.19	66	0.000020	<0.01	10.286	0.110	0.0594	0.0004	0.0973	0.0011						598	6			
9.2	128	29	0.23	20	0.000066	0.10	5.482	0.068	0.1103	0.0009	0.1822	0.0023	2.749	0.042	0.1094	0.0010	0.817	1079	12	1790	16	40
10.1	841	103	0.12	70	0.000037	<0.01	10.337	0.110	0.0595	0.0004	0.0968	0.0011						595	6			
11.1	930	217	0.23	75	0.000007	0.04	10.723	0.115	0.0595	0.0004	0.0932	0.0010						575	6			
12.1	705	691	0.98	60	0.000029	<0.01	10.108	0.120	0.0599	0.0004	0.0990	0.0012						608	7			
13.1	1977	806	0.41	165	0.000051	0.02	10.264	0.106	0.0601	0.0002	0.0974	0.0010						599	6			
14.1	854	226	0.26	72	0.000032	0.13	10.197	0.108	0.0610	0.0007	0.0979	0.0011						602	6			
15.1	1312	124	0.09	109	0.000009	<0.01	10.308	0.108	0.0598	0.0003	0.0970	0.0010						597	6			

1. Uncertainties given at the one σ level.
2. Error in FC1 reference zrn calibration was 0.59% for the analytical session (not included in above errors but required when comparing 206Pb/238U data from different mounts).
3. f_{206} % denotes the percentage of ^{206}Pb that is common Pb.
4. For areas older than ~800 Ma correction for common Pb made using the measured $^{204}Pb/^{206}Pb$ ratio following Tera and Wasserburg (1972) as outlined in Williams (1998).
5. For areas younger than ~800 Ma correction for common Pb made using the measured $^{238}U/^{206}Pb$ and $^{207}Pb/^{206}Pb$ ratios.
6. For % Disc, 0% denotes a concordant analysis.

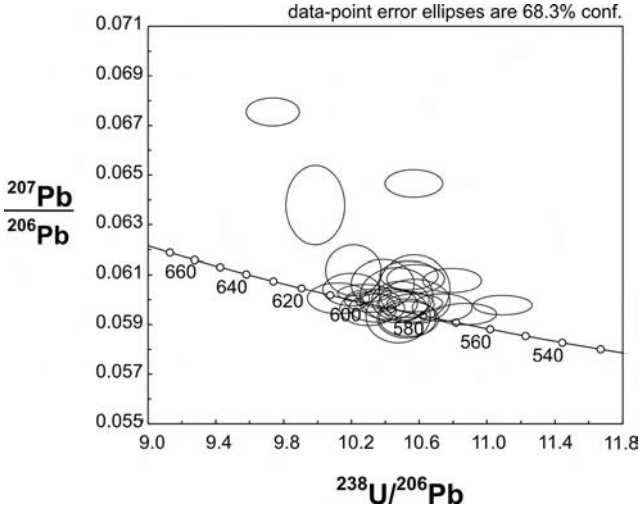

Fig. 8. Enlarged concordia plot of SHRIMP analyses (after Terra & Wasserburg, 1972) for zircon overgrowths and individual zircon crystals from the Nowolesie gneiss at Skalice (sample S6). Concordia shows the total Pb/Pb ratios vs. the calibrated U/Pb ratios, uncorrected for common Pb. Analyses are plotted as 1σ error ellipses.

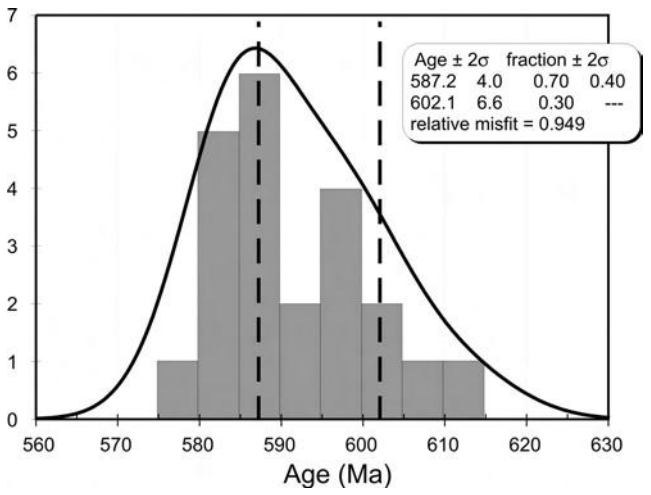

Fig. 9. Plot of probability density with stacked histogram (using the Isoplot/Ex program by Ludwig, 1999) of the radiogenic Pb/U ages for the Neoproterozoic overgrowths and individual zircon crystals from the Nowolesie gneiss at Skalice (sample S6).

core-absent zircon crystals with grain size, and between the size of the zircons with cores and the ages of the cores. The cores of the finer crystals are clearly younger than those of the coarser zircons (Table 1).

In some "whitened" core-absent zircons, the U/Pb ages and Th/U ratios were obtained for both central and marginal parts of the crystals (Table 1; Fig. 4: 17, 20). The calculated age differences are less than a few million years, and the Th/U ratios are roughly the same (0.17–0.23). This is in contrast to the zircons with cores, where both the age differences and Th/U ratio scatter are much larger (Table 1).

Exceptionally, among the CL "whitened" zircons with remnant "ghost" zonation, we find zircons with a greater age difference and with more significant differences in the Th/U ratios between the core and rim of the crystals (Table 1, points 7.1 & 7.2 from the finer fraction; Fig. 4: 15), in spite of the lack of a distinct core. Such "whitening" of the external parts of the overgrowths, with or without the "ghost" zonation, are usually interpreted as an effect of annealing (e.g. Schaltegger *et al.*, 1999; Silva *et al.*, 2000) or as the result of recrystallization of an originally zoned zircon (e.g. Nemchin & Pidgeon, 1997).

The reduction of the weighted means was done after rejecting extreme $^{206}Pb/^{238}U$ values in both the grain-size fractions (Klimas, 2008). The resultant weighted mean ages are 588.9 ± 4.6 Ma for the coarser fraction and 601.7 ± 4.4 Ma for the finer fraction. Two additional corrections to these weighted means were made due to the wrong grain-size classification of two crystals: the very long-prismatic crystal of grain 12.1 and an age of 591.4 ± 6.2 Ma (Table 1, Fig. 4: 8) should have been included in the finer fraction; grain 1.1 with an age of 580.0 ± 6.0 Ma should have been in the coarser fraction (Table 1, Fig. 4: 28).

The age of broken grain 11.1 (Fig. 4: 21) from the coarser fraction was calculated to be 570.8 ± 5.9 Ma. However, this grain was excluded from the weighted mean age of the whole population due to cracks visible in the crystal that could have caused Pb loss. After these corrections, the weighted mean $^{206}Pb/^{238}U$ ages are close to 600 Ma for the fine grain size and 585 Ma for the coarser grain size.

Both age groups of zircons can be found in one gneiss sample. However, among the 27 analyses performed on overgrowths and core-absent grains, no crystals were found with the "triple history" of an old core mantled with the internal overgrowth of ~600 Ma followed, in turn, by an external rim of ~585 Ma. A few crystals did exhibit three different zones under CL, but they could not be analyzed due to their small thickness (below 20 μm; Fig. 4: 7) or because of signs of metamictization.

DISCUSSION AND CONCLUSION

ORIGIN OF THE NOWOLESIE GNEISS

Based on petrography and zircon analyses, the Nowolesie gneiss can be interpreted as migmatized metapelites that contain admixtures of psammitic and magmatic materials.

Despite the roundness of most of the Palaeo- and Mesoproterozoic zircon cores from the Nowolesie gneiss, it is still possible to decipher their magmatic derivation via their oscillatory zonation and relatively high Th/U ratios (Table 1, Fig. 5). Based on the typology of zircon cores,

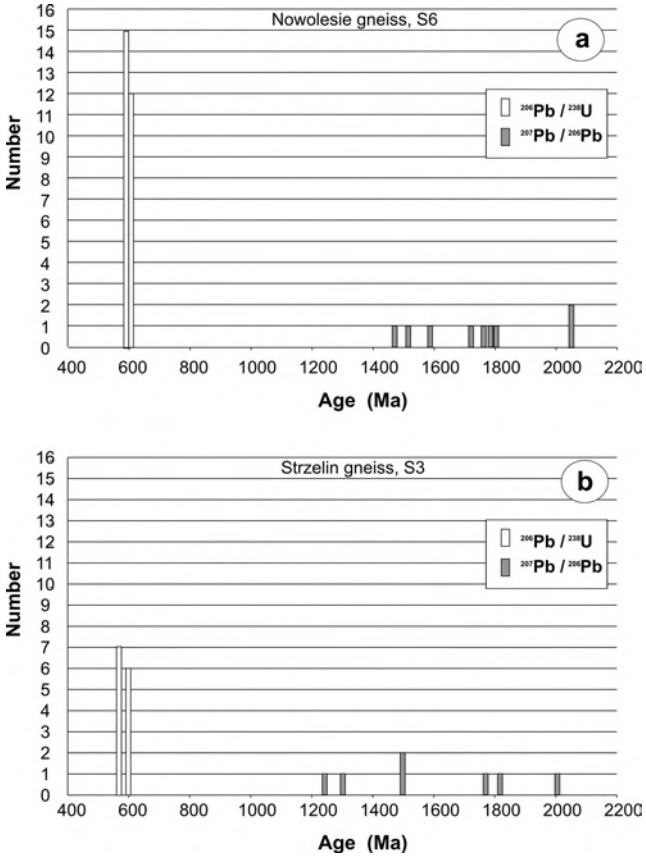

Fig. 10. Histograms of the U–Pb ages for (a) the zircons from the Nowolesie gneiss (sample S6); and (b), the Strzelin gneiss (sample S3).

these gneisses probably contain contributions from calc-alkaline to alkaline magmas. Any detrital component could have come from anorthosites, charnockites, tonalite–trondhjemite–granodiorite assemblages and alkaline granitoids, all of which were common in the Proterozoic. Granulites, migmatites and various gneisses could have been the source for the unzoned zircon cores, which often display evidence of corrosion and recrystallization. The CL-bright unzoned cores could also have derived from a magmatic source, but had lost their zonation as a result of secondary processes (metamorphism, fluid activity etc.).

The distribution of zircon core ages lie mainly within the Palaeo- and Mesoproterozoic. The lack of Grenvillian (1.3–0.9 Ga) and younger inheritance ages in the Nowolesie gneiss makes these zircons similar to those in the Strzelin gneiss from Dębniki (Figs. 10 & 11). However, there are some differences in the inherited ages in these two gneisses: the Strzelin gneiss contains grains that are ~1.2–1.3 Ga, and such grains are not found in the Nowolesie gneiss.

Furthermore, global palaeogeographic correlations are not yet accurate enough to give unequivocal source areas: zircons from around 1.7–2.1 Ga have been reported from both the West African and Amazonian cratons (and to a limited extent from Baltica), whereas younger zircons, aged between 1.2 and 1.6 Ga, are more characteristic only of the Amazonian craton (Zeh *et al.*, 2001). More reliable correlations, possibly involving other source areas (e.g. East Africa, Baltica) would require more geochronological data from the gneisses.

It is not certain when and how many migmatization events the Nowolesie gneiss experienced. Based on the new SHRIMP data, two Neoproterozoic anatectic zircon generations were recognised, differing in age by ~15 Ma. They may represent two distinct migmatization events, at 602 ± 7 Ma and 587 ± 4 Ma, respectively (Fig. 10). Both these dates fall within the range of ages obtained by various methods from gneisses of the Brunovistulian Terrane, where regional metamorphism and plutonic activity have been linked to two phases of the Cadomian tectonothermal cycle (Finger *et al.*, 2000). A similar time gap of 32 Ma was found in the Strzelin gneiss from Dębniki (Oberc-Dziedzic *et al.*, 2003b, 2005; Klimas, 2008) and suggests a two-stage tectonothermal event.

In the younger generation of zircons from the Nowolesie gneiss, fragments of large broken magmatic euhedral and oscillatory zoned zircons were dated. Apart from that, a suite of diversified CL-"whitened" zircons have been found, with clear symptoms of recrystallization and fluid activity that largely erased their zonation and, possibly, caused their rejuvenation. Both these types of zircons could have been derived from separate magmatic sources and subsequently "juxtaposed" with the anatectic zircons. Possibly, some of the magmatic zircons might have been product of synsedimentary volcanic activity.

We cannot preclude that the Nowolesie gneiss did not also experience anatectic pulses during the Variscan tectono-metamorphic reconstruction (Oberc-Dziedzic, 1995) but, to date, no Variscan-age zircons have been found. Perhaps newly formed anatectic melt was quickly segregated and pressed out of the source rock, the remaining residuum not having the Zr saturation levels necessary for new zircon to crystallize during the Variscan orogeny. Such quickly removed melts, however, usually leave their trace in the form of overgrowths and needle-like, long-prismatic zircons (e.g. Schaltegger *et al.*, 1999). Such grains were observed from the Nowolesie gneiss but these probably document the younger of the two Neoproterozoic anatectic events, the one at 587 ± 4 Ma (Fig. 4: 24).

The small number of zircon crystals in the Nowolesie gneiss as well as the low Zr concentration in the bulk rock (58 ppm reported in Oberc-Dziedzic *et al.*, 2005) are also important diagnostic features. They may indicate that the gneiss protoliths were poor in zircon or that the early formed anatectic melt had separated from a Zr-rich residuum.

A significant feature of the zircons of this study is the lack of evidence of a "triple history" in their interiors, which would record a sequence of three, or more, sequential overgrowths. The older zircons, 602 ± 7 Ma in age, are smaller and are concentrated mainly in the finer-grained fraction. The younger zircons of 587 ± 4 Ma are mostly larger (0.12–0.20 mm). On the other hand, the ages of zircon cores in the coarser fraction are, in general, older, compared to those in the finer fraction, even after rejecting the points with relatively high discordance (Table 1).

The two Neoproterozoic tectonothermal events are reflected not only by thin overgrowths with planar zoning

on older cores, but also as individual crystals without cores. Their forms and internal structures suggest that most did not originate from subsolidus nucleation and crystallization. The dominant grains with over- growths of the two age generations show features typical of zircons that crystallized from an anatectic melt (e.g. Vavra *et al.*, 1996; Vavra *et al.*, 1999; Schaltegger *et al.*, 1999). Zircon grains with two generations of overgrowths may represent two pulses of crustal anatexis that selectively operated in the metasedimentary rocks. It is not clear why only part of any given zircon, and in particular those in the fine-grained size fraction (0.06–0.12 mm), got older over-growths. It is also not clear why younger over- growths did not form around the older overgrowths and why the younger overgrowths are found mainly in the coarser-grained fraction (0.12–0.20 mm).

It seems quite probable that the Nowolesie gneiss underwent a two-stage partial melting. The cause of this could either be from changing the bulk physical and chemical conditions of anatexis – T, P, composition, fluid activities etc. – or it could result from selective melting whereby parts of zircons were selectively protected within minerals that did not take part in the anatexis. Furthermore, Ostwald ripening could have operated as a differentiating factor between older, smaller zircons and younger, larger crystals, because this ripening process allows larger crystals to grow at the expense of the smaller ones during anatexis (Nemchin *et al.*,2001; Montero *et al.*, 2004).

Although the observed age differences between zircon crystals may simply reflect radiogenic Pb^*-loss in some of the zircons it seems most likely, in the Nowolesie gneiss, to have resulted from a combination of the factors mentioned above. This latter possibility is confirmed by core-absent crystals of the age of ~587 ± 4 Ma that comprise many euhedral forms with oscillatory magmatic zoning but showing clear notching along edges and corners, as well as broken fragments of large crystals. These defects could have resulted from both sedimentary and tectonic processes but may also indicate an admixture of volcanic material. The often observed CL-"whitenings" of selected zoning layers often signify effects of subsequent fluid actions that may also cause Pb^*-loss.

Based on the petrographic evidence of this study, and comparing the Nowolesie gneiss with similar rocks of the migmatitic dome of St. Malo, France, (Milord *et al.*, 2001, fig. 11, therein), we can recognize, in the Nowolesie gneiss, examples of both mesocratic diatexites with large portions of melt and metatexites with small portions of melt that show signs of solid-rock rheology. Sample S6 can be interpreted as a mesocratic diatexite with a banded structure. This rock type may have formed by new melt that had separated from a relatively zircon-rich residuum, penetrating into and capturing fragments of both the residuum and the mesosomatic components that themselves were the result of incongruent melting of the gneiss protolith. The components of the palaeosome comprised zircon, biotite and some plagioclase, especially the Ca-rich variety of ~An_{40} (Wojnar, 1995). The newly formed melt was partially segregated in the form of leucosomes and small veins and nests. Among the Nowolesie gneiss are also migmatites showing stromatitic and nebulitic structures (Oberc-Dziedzic, 1995).

REGIONAL CORRELATIONS AND TECTONIC IMPLICATIONS

The new SHRIMP results presented here have implications for the regional geology of the eastern part of the Fore-Sudetic Block, and in particular may contribute to the discussion on the location of the extension of the Moldanubian Thrust Zone within that block (cf. Oberc-Dziedzic & Madej, 2002; Oberc-Dziedzic *et al.*, 2005).

The gneisses of the Strzelin Massif, as a whole, have previously been assigned to the Proterozoic (e.g. Oberc, 1966, 1972, 1975), but only recently could this be proved by geochronological studies. The Gościęcice gneiss from the Strzelin Massif was the first to be dated and it yielded a U–Pb evaporation multigrain zircon age of 504 ± 3 Ma (Oliver *et al.*, 1993). This date was then refined using the single-grain evaporation method to 513 ± 1 Ma (Kröner & Mazur, 2003).

The previous SHRIMP zircon ages of 600 ± 7 Ma and 568 ± 7 Ma reported from the Strzelin gneiss (Oberc-Dziedzic *et al.*, 2003b) when allied with the 602 ± 7 Ma and 587 ± 4 Ma ages from the Nowolesie gneiss in this study provide firm geochronological evidence for Neoproterozoic tectonothermal event(s) recorded in the gneisses of the NE part of the Fore-Sudetic Block.

The zircons from the Strzelin and Nowolesie gneiss often contain older cores and younger, usually thin overgrowths. The SHRIMP dating of these overgrowths in zircons from the Nowolesie gneiss allowed to correct substantially the earlier date of 1.020 ± 1 Ma (Kröner & Mazur, 2003). As a consequence, the ages of zircons from the Nowolesie gneiss, only a little older than those from the Strzelin gneiss, fit more reasonably with a regional geological model in which both gneisses belong to the lower part of the tectonostratigraphic column (Fig. 11).

The $^{206}Pb/^{238}U$ SHRIMP ages of 500 ± 5 Ma from zircons of the pale Stachów gneiss (Oberc-Dziedzic *et al.*, 2005; Klimas, 2008), together with the earlier published ages of 504 ± 3 Ma from the Gościęcice gneiss (Oliver *et al.*, 1993) help to distinguish local Neoproterozoic from Lower Palaeozoic gneisses. The ability to now separate different gneisses may also help to distinguish between the different gneiss complexes of the two major crustal units: the Moldanubian and Saxo-Thuringian Zones of the Bohemian Massif and the Brunovistulian Terrane, both being separated by the Moldanubian Thrust Zone (Franke & Żelaźniewicz, 2000, 2002; Schulmann & Gayer, 2000; Aleksandrowski & Mazur, 2002). A diagnostic difference seems to be that the Brunovistulian unit has an abundance of ~630–570 Ma gneisses, whereas the Moldanubian/Saxo-Thuringian unit is dominated by ~500 Ma gneisses (Finger *et al.*, 2000; Oberc-Dziedzic *et al.*, 2003b, 2005). Thus, the Nowolesie and Strzelin gneisses seem to correlate with similar gneisses of the Cadomian Brunovistulian basement; the Gościęcice gneiss and the Stachów and Henryków gneisses of the Stachów complex correlate

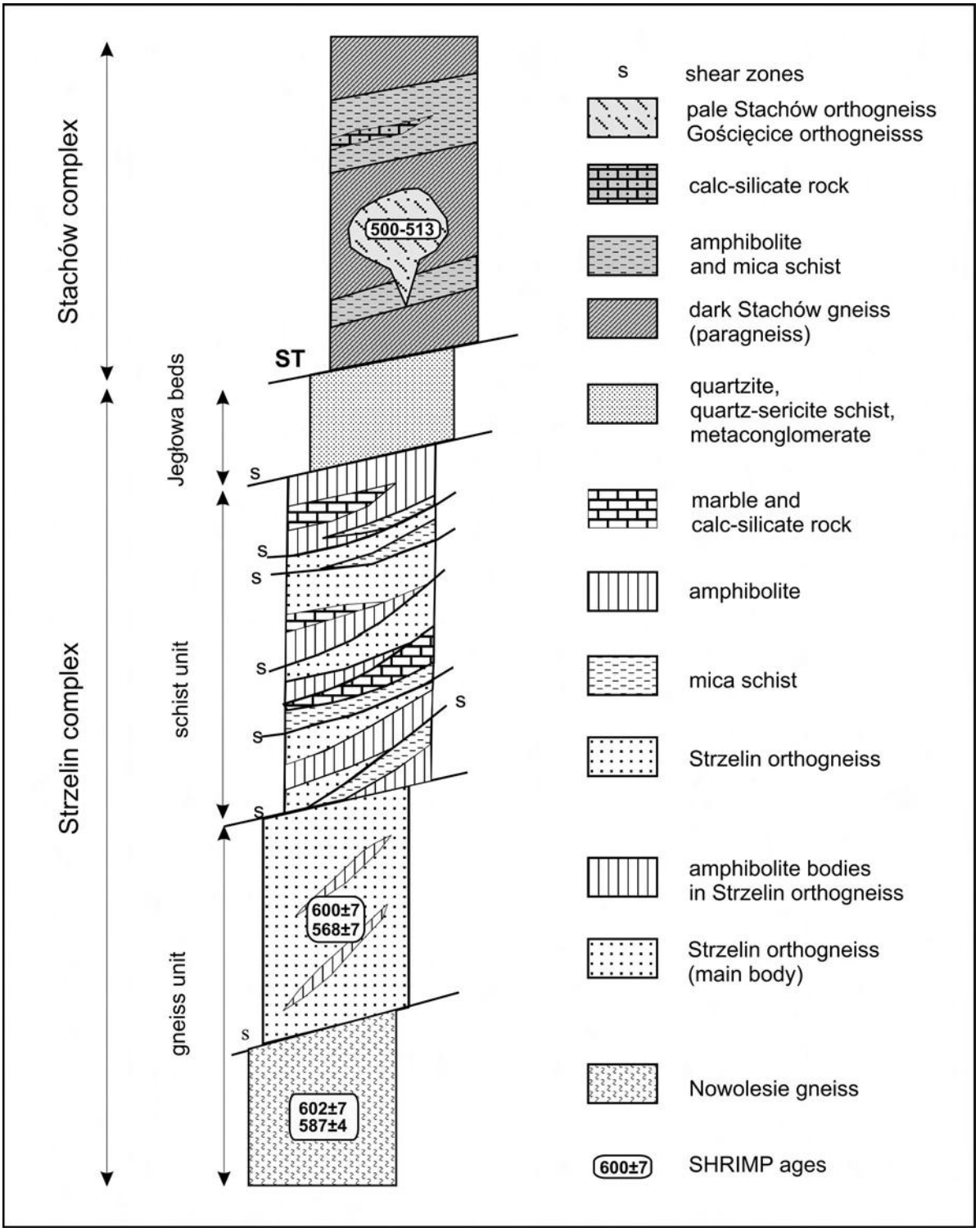

Fig. 11. Simplified log of the lithological subdivisions of the Strzelin and Stachów complexes (modified after Oberc-Dziedzic *et al.*, 2005). Map incorporates the new U–Pb data.

with gneisses in the Moldanubian and Saxo-Thuringian zones (Oberc-Dziedzic *et al.*, 2003b, 2005; Klimas, 2008; cf. Figs. 1 & 10).

Thus, all the SHRIMP zircon data demonstrate that there are reasonably distinct and characteristic zircon populations from the gneisses within the Brunovistulian and the Moldanubian/Saxo-Thuringian tectonostratigraphic units. In particular, the Nowolesie and Strzelin gneisses are associated with the Brunovistulian; the pale Stachów gneiss correlate with the Moldanubian/Saxo-Thuringian. The nature of the distinction between the zircon populations can be seen in the ages of the main zircon population overgrowths and the core-absent crystals, and also in the ages of the older cores (Fig. 10). The older gneisses seem to

have mostly sedimentary-derived zircon cores that are Palaeo- and Mesoproterozoic in age. The younger gneisses, such as the Stachów gneiss, commonly contain Neoproterozoic zircon cores.

In summary, the new SHRIMP zircon data from the Nowolesie gneiss supplied further evidence for the age and provenance of a variety of gneisses that are exposed in the eastern part of the FSB. The detailed study of this gneiss provided information about the Palaeoproterozoic and Mesoproterozoic ages of the inherited zircons. These ages suggest Gondwana (the West African craton and/or the Amazonian craton) as a possible source area. The major zircon populations in the Nowolesie gneiss document intense metamorphic and anatectic tectonothermal events during the Neoproterozoic, notably at around 602 ± 7 Ma and at 587 ± 4 Ma. Consequently, the Nowolesie gneiss can be correlated with gneisses that are widespread throughout the Brunovistulian Terrane and can also be interpreted as being located on the eastern side of the northern extension of the Moldanubian Thrust Zone (cf. Oberc-Dziedzic *et al.*, 2005).

Acknowledgements

The study was supported from the internal grants of the University of Wrocław, 2022/W/ING and 1017/S/ING. Teresa Oberc-Dziedzic is thanked for help, co-operation and fruitful discussions on the geology and petrology of the Strzelin and Lipowe Hills massifs. Kalina Dymna and Henryk Siagło helped efficiently in zircon separation. Vaclav Kachlik, Patrick Roycroft and Andrzej Żelaźniewicz are thanked for their constructive reviews and corrections.

REFERENCES

ACHRAMOWICZ, S., MUSZYŃSKI, A. & SCHLIESTEDT, M., 1996. Metamorfizm skał wapienno-krzemianowych obszaru Wzgórz Strzelińskich – kontekst geotektoniczny. [Metamorphism of the calc-silicate rocks from the Wzgórza Strzelińskie region]. *Polskie Towarzystwo Mineralogiczne, Prace Specjalne*, 8: 8–10.

ALEKSANDROWSKI, P., KRYZA, R., MAZUR, S., PIN, C. & ZALASIEWICZ, J.A., 2000. The Polish Sudetes: Caledonian or Variscan? *Transactions of the Royal Society of Edinburgh, Earth Sciences*, 90: 127–146.

ALEKSANDROWSKI, P. & MAZUR. S., 2002. Collage tectonics in the north easternmost part of the Variscan Belt: the Sudetes, Bohemian Massif. In: J.A. Winchester, T.C. Pharaoh, & J. Verniers (Eds). *Palaeozoic Amalgamation of Central Europe*. Geological Society, London, Special Publications, 201: 237–277.

BADURA, J., 1979. *Szczegółowa mapa geologiczna Sudetów. Arkusz Stolec, 1:25000*. Instytut Geologiczny, Wydawnictwa Geologiczne.

BARANOWSKI, Z., HAYDUKIEWICZ, A., KRYZA, R., LORENC, S., MUSZYŃSKI, A., SOLECKI, A. & URBANEK, Z., 1990. Outline of the geology of the Góry Kaczawskie (Sudetes, Poland). *Neues Jahrbuch für Geologie und Paläontologie*, 179: 223–257.

BEDERKE, E., 1929. Die Grenze von Ost- und Westsudeten und ihre Bedeutung für die Einordnung der Sudeten in den Gebirgsbau Mitteleuropas. *Geologische Rundschau*, 20: 186–205.

BENISEK, A. & FINGER, F., 1993. Factor controlling the development of prism faces in granite zircons: a microprobe study. *Contributions to Mineralogy and Petrology*, 114: 441–451.

BEREŚ, B., 1969. Petrografia granitu Strzelina i okolicy. *Acta Geologica Polonica*, 28: 5–105.

COLLINS, A.S., KRYZA, R. & ZALASIEWICZ, J.A., 2000. Macrofabric fingerprints of Late Devonian – Early Carboniferous subduction in the Polish Variscides, the Kaczawa Complex, Sudetes. *Journal of the Geological Society, London*, 157: 238–288.

CORFU, F., HANCHAR, J.M., HOSKIN, P.W.O. & KINNY, P., 2003. Atlas of zircon textures. In: Hanchar, J.M. & Hoskin, P.W.O. (Eds). *Zircon*. Reviews in Mineralogy and Geochemistry, 53: 469–500. Mineralogical Society of America & Geochemical Society, Washington, DC.

CYMERMAN, Z., 1993a. Czy w Sudetach istnieje nasunięcie ramzowskie? [Does the Ramzova Thrust exist in the Sudetes?]. *Przegląd Geologiczny*, 41: 700–706.

CYMERMAN, Z.,1993b. Jednostki tektoniczne metamorfiku strzelińskiego w świetle nowej analizy strukturalnej (Dolny Śląsk). [Tectonic units of the Strzelin metamorphicum in the light of new structural analyses (Lower Silesia)]. *Przegląd Geologiczny*, 41: 421–427.

CYMERMAN, Z., PIASECKI, M.A.J. & SESTON, R., 1997. Terranes and terrane boundaries in the Sudetes, northeast Bohemian Massif. *Geological Magazine*, 134: 717–725.

CYMERMAN, Z. & PIASECKI, M.A.J., 2004. The terranes concept in the Sudetes, Bohemian Massif. *Geological Quarterly*, 38: 191–210.

CWOJDZIŃSKI, S. & ŻELAŹNIEWICZ, A., 1995. Podłoże krystaliczne bloku przedsudeckiego. [Crystalline basement of the Fore-Sudetic Block]. *Przewodnik LXVI Zjazdu PTG*: 11–126.

DALLMEYER, R.D., NEUBAUER, F. & HÖCK, V., 1992. $^{40}Ar/^{39}Ar$ mineral age controls on the chronology of late Palaeozoic tectonothermal activity in the Southeastern Bohemian Massif, Austria Moldanubian and Moravo-Silesian Zones. *Tectonophysics*, 210: 135–153.

DA SILVA, L.C., HARTMANN, L.A., MCNAUGHTON, N.J. & FLETCHER, I., 2000. Zircon U–Pb SHRIMP dating of a Neoproterozoic overprint in Paleoproterozoic granitic-gneissic terranes, southern Brazil. *American Mineralogist*, 85: 649-667.

DAVIS, D.W., WILLIAMS, I.S. & KROGH, T.E., 2003. Historical development of zircon geochronology. In: Hanchar, J.M. & Hoskin, P.W.O. (Eds). *Zircon*. Reviews in Mineralogy and Geochemistry, 53: 145–181. Mineralogical Society of America & Geochemical Society, Washington, DC.

DON, J., 1990. The differences in Palaeozoic facies – structural evolution of the West Sudetes. *Neues Jahrbuch für Geologie und Paläontologie*, 179: 307–328.

DUDEK, 1980. The crystalline basement blocks Carpathians in Moravia-Brunovistulicum. *Rozpravy Aeskoslovenskë Akademie Vëd, Rada Matematických a Přírodnich Vëd*, 90: 1–85.

FINGER, F., HANŽL, P., PIN, C., VON QUADT, A., & STEYRER, H.P., 2000. The Brunovistulian: Avalonian Precambrian sequence at the Eastern and of the Central Euro-

pean Variscides? In: Franke, W., Haak, V., Oncken, O. & Tanner, D. (Eds). *Orogenic Processes: Quantification and Modelling in the Variscan Belt*. Geological Society, London, Special Publications, 179: 103–112.

FRANKE, W., ŻELAŹNIEWICZ, A., PORĘBSKI, S.J. & WAJSPRYCH, B., 1993. Saxothuringian Zone in Germany and Poland: differences and common features. *Geologische Rundschau*, 82: 583–599.

FRANKE, W. & ŻELAŹNIEWICZ, A., 2000. The eastern termination of the Variscides: terrane correlation and kinematics evolution. In: Franke, W., Haak, V., Oncken, O., & Tanner, D. (Eds). *Orogenic Processes: Quantification and Modelling in the Variscan Belt*. Geological Society, London, Special Publications, 179: 63–86.

FRANKE, W. & ŻELAŹNIEWICZ, A., 2002. Structure and evolution of the Bohemian Arc. In: Winchester, J.A., Pharaoh, T.C. & Verniers, J. (Eds). *Palaeozoic Amalgamation of Central Europe*. Geological Society, London, Special Publications, 201: 279–293.

FRIEDL, G., FINGER, F., PAGUETTE, J.L., VON QUADT, A., MCNAUGHTON, N.J. & FLETCHER, I.R., 2004. Pre-Variscan geological events in the Austrian part of the Bohemian Massif deduced from U-Pb zircon ages. *International Journal of Earth Sciences*, 93: 802–823.

GIACOMINI, F., BRAGA, R., TIEPOLO, M. & TRIBUZIO, R., 2007. New constrains on the origin and age of Variscan eclogitic rocks (Liguria Alps, Italy). *Contributions to Mineralogy and Petrology*, 153: 29–53.

GUILLOT, F., SCHALTEGGER, U., BERTRAND, J.M., DELOULE, E. & BAUDIN, T., 2002. Zircon U-Pb geochronology of Ordovician magmatism in the polycyclic Ruitor Massif (Internal W Alps). *International Journal of Earth Sciences*, 91: 964-978.

HACKER, R.B., RATSCHBACHER, L., WEBB, L., IRELAND, T., WALKER, D. & SHUWEN, D., 1998. U/Pb zircon ages constrain the architecture of the ultrahigh-pressure Qinling-Dabie Orogen, China. *Earth and Planetary Science Letters*, 161: 215–230.

HANCHAR, J.M. & HOSKIN, P.W.O., 2003. Zircon. In: Hanchar, J.M. & Hoskin, P.W.O. (Eds). *Zircon*. Reviews in Mineralogy and Geochemistry, 53: Preface, v-vii. Mineralogical Society of America & Geochemical Society, Washington, DC.

HOSKIN, P.W.O., 2000. Patterns of chaos: fractal statistics and the oscillatory chemistry of zircon. *Geochimica et Cosmochimica Acta*, 64: 1905–1923.

HOSKIN, P.W.O. & SCHALTEGGER, U., 2003. The composition of zircon and igneous and metamorphic petrogenesis. In: Hanchar, J.M. & Hoskin, P.W.O. (Eds). *Zircon*. Reviews in Mineralogy and Geochemistry, 53: 27–62. Mineralogical Society of America & Geochemical Society, Washington, DC.

KEMPE, U., GRUNER, T., NASDALA, L. & WOLF, D., 2000. Relevance of cathodoluminescence for the interpretation of U-Pb zircon ages, with an example of an application to a study of zircons from the Saxonian Granulite Complex, Germany. In: Pagel, M., Barbin, V., Blanc, P., & Ohnenstetter, D. (Eds). *Cathodoluminesence in Geosciences*. Springer, Berlin, Heidelberg, New York, pp. 415–455.

KLIMAS K., 2008: Geochronologia i petrogenetyczne studium cyrkonów z wybranych skał krystalicznych wschodniej części bloku przedsudeckiego. [A geochronologic and petrogenetic study of zircons from selected crystalline rocks in the eastern part of the Fore-Sudetic Block]. Uniwersytet Wrocławski, ARGO, Wrocław. 1–194.

KLIMAS, K. & SZCZEPAŃSKI, J., 2005: Needle-like zircons of selected crystalline rocks from eastern part of the Fore-Sudetic Block (SW Poland): good tracers for dating rapid tectonothermal events. *Polskie Towarzystwo. Mineralogiczne, Prace Specjalne*, 25: 122–125.

KLIMAS-AUGUST, K., 1989. Geneza gnejsów i granitów wschodniej części metamorfiku izerskiego w świetle badań cyrkonu w wybranych profilach geologicznych. [Genesis of gneisses and granites from the eastern part of the Izera metamorphic complex in the light of study on zircon from selected geological profiles]. *Geologia Sudetica*, 24: 1–99.

KOSSMAT, F., 1927. Gliederung des varistischen Gebirgsbaues. *Abhandlungen Sächsischen Geologischen Landesamts*, 1: 1–39

KRÖNER, A. & MAZUR, S., 2003. Proterozoic and Palaeozoic crustal components across the East/Central Sudetes boundary at the eastern margin of the Bohemian Massif: new U/Pb and Pb/Pb single zircon ages from the eastern Fore-Sudetic block (SW Poland). *Journal of the Czech Geological Society*, 48: 83–84.

KRYZA, R., PIN, C. & VIELZEUF, D., 1996. High-pressure granulites from the Sudetes (south-west Poland): evidence of crustal subduction and collisional thickening in the Variscan Belt. *Journal of Metamorphic Geology*, 14: 531–546.

KRYZA, R., MAZUR, S. & OBERC-DZIEDZIC, T., 2004. The Sudetic geological mosaic: Insights into the root of the Variscan orogen. *Przegląd Geologiczny*, 52: 761–773.

KRYZA, R. & FANNING, C.M., 2007: Devonian deep-crustal metamorphism and exhumation in Variscan Orogen: evidence from SHRIMP zircon ages from the HT-HP granulites and migmatites of the Góry Sowie (Polish Sudetes). *Geodinamica Acta*, 20: 159–175.

KRYZA, R. & ZALASIEWICZ, J., 2008. Records of Precambrian-Early Palaeozoic volcanic and sedimentary processes in the Central European Variscides: A review of SHRIMP zircon data from the Kaczawa succession (Sudetes, SW Poland). *Tectonophysics*, 461: 60–71.

LIU, F., LIOU, J.G. & XU, Z., 2005. U–Pb SHRIMP ages recorded in the coesite-bearing zircon domain of paragneisses in the southwestern Sulu terrane, eastern China: New interpretation. *American Mineralogist*, 90: 790–800.

LUDWIG, K.R., 1999. *Using Isoplot/Ex, version 2.01. A geochronological toolkit for Microsoft Excel*. Berkeley Geochronology Center, Special Publication No 1a, 47pp, Berkeley CA.

MAJEROWICZ, A., 1975. Cyrkony niektórych skał krystalicznych jako wskaźniki petrogenetyczne. [Zircons from some crystalline rocks as petrogenetic indicators]. *Acta Universitatis Wratislaviensis*, 247, Pr. Geol.-Miner., 4.

MATTE, P., MALUSKI, H., REJLICH, P. & FRANKE, W., 1990. Terrane boundaries in the Bohemian Massif: Results of large scale Variscan shearing. *Tectonophysics*, 177: 151–170.

MAZUR, S., ALEKSANDROWSKI, P., KRYZA R. & OBERC-DZIEDZIC T., 2006. The Variscan Orogen in Poland. *Geological Quarterly*, 50: 89–118.

MILORD, I., SAWYER, E.W. & BROWN, M., 2001. Formation of diatexite migmatite and granite magma during anatexis of semi-pelitic metasedimentary rocks: an example from St. Malo, France. *Journal of Petrology*, 42: 487–505.

MONTERO, P., BEA, F., ZINGER, T.F., SCARROW, J.H., MOLINA, J.F. & WHITEHOUSE, M., 2004. 55 milion years of continuous anatexis in Central Iberia: single-zircon dating of the Peña Negra Complex. *Journal of the Geological Society, London*, 161: 255–263.

NEMCHIN, A.A. & PIDGEON, R.T., 1997. Evolution of the Darling Range Batholith, Yilgarn Craton, Western Australia: a SHRIMP zircon study. *Journal of Petrology*, 38: 625–649.

NEMCHIN, A.A, GIANNINI, L.M., BODORKOS, S. & OLIVER, N.H.S., 2001. Ostwald ripening as a possible mechanism for zircon overgrowth forming during anatexis: theoretical constraints, a numerical model and its application to pelitic migmatites of the Tickalara Metamorphics, northwestern Australia. *Geochimica et Cosmochemica Acta*, 65: 2771–2787.

OBERC, J., 1957. Zmiany kierunków nacisków górotwórczych w strefie Sudetów zachodnich i wschodnich. [Directions of orogenic stresses in the border zone of Eastern and Western Sudetes]. *Acta Geologica Polonica*, 7: 1–27.

OBERC, J., 1966. Geologia krystaliniku Wzgórz Strzelińskich. [Geology of crystalline rocks of the Wzgórz Strzelińskie Hills, Lower Silesia]. *Studia Geologica Polonica*, 20: 1–187.

OBERC, J., 1968. Granica między strukturą zachodnio i wschodniosudecką. [The boundary between the western and eastern Sudetic tectonic structure]. *Rocznik Polskiego Towarzystwa Geologicznego*, 38: 203–271.

OBERC, J., 1972. Budowa geologiczna Polski, t. IV, Tektonika cz.2, Sudety i obszary przyległe. [Geological structure of Poland, t. IV, Tectonics p. 2, Sudetes and adjacent areas]. Wydawnictwa Geologiczne. Warszawa: 3–307.

OBERC, J., 1975. Tektonika i rozwój wschodniej części bloku przedsudeckiego. [Tectonics and development eastern part of the Fore-Sudetic Block]. *Przegląd Geologiczny*, 2: 213-220.

OBERC, J., 1988. Tektonika metamorfiku Wzgórz Strzelińskich. [Tectonics of the Wzgórza Strzelińskie metamorphicum]. *Materiały do sesji naukowej: Budowa, rozwój i surowce skalne krystaliniku strzelińskiego.* Instytut Nauk Geologicznych Uniwersytetu Wrocławskiego, Przedsiębiorstwo Geologiczne Wrocław, pp 32–41.

OBERC, J. (Ed), with OBERC-DZIEDZIC, T. & KLIMAS-AUGUST, K., 1988. *Mapa geologiczna Wzgórz Strzelińskich w skali 1:25 000*. [*Geological map of the Strzelin Massif at scale 1: 25 000*]. Instytut Nauk Geologicznych Uniwersytetu Wrocławskiego, Przedsiębiorstwo Geologiczne Wrocław.

OBERC-DZIEDZIC, T., 1988. Geologia krystaliniku Wzgórz Strzelińskich. [Geology of the Wzgórza Strzelińskie crystallinicum]. Annales Societas Geologorum Poloniae, *Przewodnik do LXVI zjazdu PTG*: 111–126.

OBERC-DZIEDZIC, T., 1991. Pozycja geologiczna granitoidów strzelińskich. [Geological setting of the Strzelin granitoids]. *Acta Universitatis Wratislaviensis, 1375, Prace Geologiczno-Mineralogiczne*, 29: 295–324.

OBERC-DZIEDZIC, T., 1995. Problematyka badań serii metamorficznych Wzgórz Strzelińskich w świetle materiału wiertniczego. [Investigations of the Wzgórza Strzelińskie metamorphic complex based on bore-hole material]. *Acta Universitatis Wratislaviensis* 1739. Prace Geologiczno-Mineralogiczne, 50: 77–103.

OBERC-DZIEDZIC, T., 1999: The metamorphic and structural development of gneisses and older schist series in the Strzelin crystalline massif (Fore-Sudetic Block, SW Poland). *Mineralogical Society of Poland - Special Papers*, 14: 10–21.

OBERC-DZIEDZIC, T. & SZCZEPAŃSKI, J., 1995. Geologia krystaliniku Wzgórz Strzelińskich. [Geology of the Wzgórza Strzelińskie Crystalline Massif]. *Przewodnik LXVI Zjazdu Polskiego Towarzystwa Geologicznego*, 21-24.IX.1995, Wrocław: 111–126.

OBERC-DZIEDZIC, T., PIN, C., DUTHOU J.L. & COUTURIE, J.P., 1996. Age and origin of the Strzelin granitoids (Fore-Sudetic Block, Poland): $^{87}Rb/^{86}Sr$ data. *Neues Jahrbuch für Mineralogie, Abhandlungen*, 171: 187–98.

OBERC-DZIEDZIC, T. & PIN. C., 2000. The granitoids of the Lipowe Hills (Fore-Sudetic Block) and their relationship to the Strzelin granites. *Geologia Sudetica*, 3: 17–22.

OBERC-DZIEDZIC, T. & MADEJ, S., 2002. The Variscan overthrust of the Lower Palaeozoic gneiss unit on the Cadomian basement in the Strzelin and Lipowe Hills massifs, Fore-Sudetic Block, SW Poland: is this part of the East-West Sudetes boundary? *Geologia Sudetica*, 34: 39–58.

OBERC-DZIEDZIC, T., KLIMAS, K., KRYZA, R., FANNING, C.M. & MADEJ, S., 2003a. SHRIMP zircon ages from gneisses help locate the West-East Sudetes boundary (NE Bohemian Massif, SW Poland). *Journal of the Czech Geological Society*, 48: 98.

OBERC-DZIEDZIC, T., KLIMAS, K., KRYZA, R. & FANNING, C.M., 2003b. SHRIMP U-Pb zircon geochronology of the Strzelin gneiss, SW Poland: evidence for a Neoproterozoic thermal event in the Fore-Sudetic Block, Central European Variscides. *International Journal of Earth Sciences*, 92: 701–711.

OBERC-DZIEDZIC, T., KRYZA, R., KLIMAS, K., FANNING, C.M. & MADEJ, S., 2005. Gneiss protolith ages and tectonic boundaries in the NE part of the Bohemian massif (Fore-Sudetic block, SW Poland). *Geological Quarterly*, 49: 363–378.

OLIVER, G.J.H., CORFU, F. & KROGH, T.E., 1993. U–Pb ages from SW Poland: evidence for a Caledonian suture zone between Baltica and Gondwana. *Journal of the Geological Society, London*, 150: 355–369.

PACES, J.B. & MILLER, J.D. Jr, 1993. Precise U-Pb ages of Duluth Complex and related mafic intrusions, northeastern Minnesota: Geochronological insights to physical, petrogenetic, Palaeomagnetic and tectonomagnetic process associated with the 1.1 Ga Midcontinent Rift System. *Journal of Geophysical Research*, 98: 13,997–14,013.

PANKHURST, R.J., RAPELA, C.W., FANNING, C.M. & MARQUEZ, M., 2006. Gondwanide continental collision and the origin of Patagonia. *Earth-Science Reviews*, 76: 235–257.

PIDGEON, R.T., 1992. Recrystallisation of oscillatory zoned zircon: some geochronological and petrological implications. *Contributions to Mineralogy and Petrology*, 110: 463–472.

PIDGEON, R.T., NEMCHIN, A.A. & HITCHEN, G.J., 1998. Internal structures of zircons from Archaean granites from the Darling Range batholith: implications for zircon stability and the interpretation of zircon U-Pb ages. *Contributions to Mineralogy and Petrology*, 132: 288–299.

PIDGEON, R.T., MACAMBIRA, M.J.B. & LAFON, J.M., 2000. Th–U–Pb isotopic systems and internal structures of complex zircons from an enderbite from the Pium Complex, Carajas Province, Brazil: evidence for the ages of granulite facies metamorphism and the protolith of the enderbite. *Chemical Geology*, 166: 159–171.

PIETRANIK, A. & WAIGHT, T., 2005. Sr isotopes in plagioclase from Gęsiniec Tonalite using microdrilling method (Strzelin Crystalline Massif). *Mineralogical Society of Poland - Special Papers*, 26: 231–234.

PUPIN, J.P., 1980. Zircon and granite petrology. *Contributions to Mineralogy and Petrology*, 73: 207–20.

PUPIN, J.P., 1988. Magmatic zoning of Hercynian granitoids in France based on zircon typology. *Schweizische Mineralogische und Petrographische Mitteilungen*, 65: 29–56.

PUPIN, J.P. & TURCO, G., 1972. Une typologie originale du zircon accesoire. *Bulletin de la Sociéte Française de Minéralogie et de Cristallographie*, 95: 348–359.

ROSSI, P.H., COCHERIE, A., FANNING, C.M. & DELOULE, E., 2006. Variscan to eo-Alpine events recorded in European lower-crust zircons sampled from the French Massif Central and Corsica, France. *Lithos*, 87: 235–

260.

RUBATTO, D., 2002. Zircon trace element geochemistry: partitioning with garnet and link between U–Pb ages and metamorphism. *Chemical Geology*, 184: 123–138.

RUBATTO, D. & GEBAUER, D., 2000. Use of cathodo- luminescence for U–Pb zircon dating by microprobe: some examples from the Western Alps. In: Pagel, M., Barbin, V., Blanc, P. & Ohnenstetter, D. (Eds): *Cathodoluminescence in Geosciences*, 373–400. Springer-Verlag, Berlin

RUBATTO, D., WILLIAMS, I.S. & BUICK, I.S., 2001. Zircon and monazite response to prograde metamorphism in the Reynolds Range, central Australia. *Contributions to Mineralogy and Petrology*, 140: 458–468.

SCHALTEGGER, U., FANNING, C.M., GÜNTHER, D., MAURIN, J.C., SCHULMANN K. & GEBAUER, D., 1999. Growth, annealing and recrystallization of zircon and preservation of monazite in high grade metamorphism: conventional and in-situ U–Pb isotope, cathodoluminescence and microchemical evidence. *Contributions to Mineralogy and Petrology*, 134: 186–201.

SCHERMAIER, A., HAUNSCHMID, B., SCHUBERT, G., FRASL, G. & FINGER, F., 1992. Discriminerung von S-Typ und I-Typ Graniten auf der basis zirconotypologischer Untersuchungen. *Frankfurter Geowissenschaftliche* Arbeiten, Serie A, 11: 149–153.

SCHULMANN, K. & GAYER, R., 2000. A model for a continental accretionary wedge developed by oblique collision: the NE Bohemian Massif. *Journal of the Geological Society, London*, 157: 401–16.

SKÁCEL, J., 1989. Hranice Lugika a Silezika (Stŕednich a Východnich Sudet). [The Lugian and Silesian boundary (middle and eastern Sudetes)]. *Acta Universitatis Wratislaviensis, Prace Geologiczno-Mineralogiczne*, 17: 45–55.

SUESS, F.E., 1926. *Intrusiontektonik und Wandertektonik im variszischen Gebirge*. Borntraeger, Berlin. 1–156.

SZCZEPAŃSKI, J., 2001. Warstwy z Jegłowej – zapis wielofazowej deformacji w strefie kontaktu Sudetów wschodnich i zachodnich (krystalinik Wzgórz Strzelińskich, blok przedsudecki). [Jegłowa Beds – record of polyphase deformation in the East and West Sudetes contact zone (Strzelin crystalline massif, Fore-Sudetic Block, SW Poland)]. *Przegląd Geologiczny*, 49: 63–71.

SZCZEPAŃSKI, J., 2002. The Ar/ Ar cooling ages of white micas from the Jegłowa Beds (Strzelin Massif, Fore Sudetic Block, SW Poland. *Geologia Sudetica*, 34: 1–7.

SZCZEPAŃSKI, J. & MAZUR, S., 2004. Syncollisional extension in the West/East Sudetes boundary zone (NE Bohemian Massif): structure and metamorphic record in the Jegłowa Beds from the Strzelin Massif (East Fore-Sudetic Block). *Neues Jahrbuch für Geologie und Paläontologie*, Abhandlungen, 233: 297–331.

TERRA, F. & WASSERBURG, G., 1972. U-Th-Pb systematics in three Apollo 14 basalts and the problem of initial Pb in lunar rocks. *Earth and Planetary Science Letters*, 14: 281–304.

TIMMERMANN, H., PARRISH, S.R., NOBLE, S.R. & KRYZA, R., 2000. New U–Pb monazite and zircon data from the Sudetes Mountains in SW Poland: evidence for a single-cycle Variscan orogeny. *Journal of the Geological Society, London*, 157: 265–268.

TURNIAK, K., MAZUR, S. & WYSOCZAŃSKI, R., 2000. SHRIMP zircon geochronology and geochemistry of the Orlica-Śnieznik gneisses (Variscan belt of Central Europe) and their tectonic implications. *Geodinamica Acta*, 13: 293–312.

TURNIAK, K., TICHOMIROWA, M. & BOMBACH, K., 2006. Pb-evaporation zircon ages of post-tectonic granitoides from Strzelin Massif (SW Poland). *Mineralogia Polonica - Special Papers*, 29: 212–215.

VALLEY, J.W. 2003. Oxygen isotopes in zircon. In: Hanchar, J.M. & Hoskin, P.W.O. (Eds). *Zircon*. Reviews in Mineralogy and Geochemistry, 53: 344–85. Mineralogical Society of America & Geochemical Society, Washington, DC.

VAVRA, G., 1990. On the kinematics of zircon growth and its petrogenetic significance: a cathodoluminescence study. *Contributions to Mineralogy and Petrology*, 106: 90–99.

VAVRA, G., 1994. Systematics of internal zircon morphology in major Variscan granitoid types. *Contributions to Mineralogy and Petrology*, 117: 331–344.

VAVRA, G., GEBAUER, D., SCHMID, R. & COMPSTON, W., 1996. Multiple zircon growth and recrystallization during polyphase Late Carboniferous to Triassic metamorphism in granulites of the Ivrea Zone (Southern Alps): an ion microprobe (SHRIMP) study. *Contributions to Mineralogy and Petrology*, 98: 109–121.

VAVRA, G., SCHMID, R. & GEBAUER, D., 1999. Internal morphology, habit and U–Th–Pb microanalysis of amphibolite to granulite facies zircons: geochronology of the Ivrea Zone (Southern Alps). *Contributions to Mineralogy and Petrology*, 134: 380–404.

WILLIAMS, I.S., 1998. U-Th-Pb gechronology by ion microprobe. In: McKibben, M.A., Shanks, W.C. & Ridley, W.I., (Eds.). *Applications of microanalytical techniques to understanding mineralizing processes.* Reviews in Economic Geology, 7: 1–35. Society of Economic Geologists.

WOJNAR, B., 1995. Analiza teksturalna i petrologia skał metamorficznych południowej części masywu strzelińskiego. [Structural analysis and petrology of metamorphic rocks of the southern part of the Strzelin Massif]. *Acta Unversitatis Wratislaviensis 1633, Prace Geologiczno-Mineralogiczne*, 46: 1–74.

WÓJCIK, L., 1963. *Szczegółowa mapa geologiczna Sudetów 1:25000. Arkusz Kuropatnik*. Instytut Geologiczny, Warszawa.

WÓJCIK, L., 1968. The Strzelin granitoid massif and its cover. *Biuletyn Instytutu Geologicznego 227, Z badań geologicznych na Dolnym Śląsku*, 17: 121–147.

WÓJCIK, J., 1973. *Objaśnienia do szczegółowej mapy geologicznej Sudetów 1:25 000. Arkusz Ciepłowody.* Instytut Geologiczny, Warszawa, p.1–57.

WROŃSKI, J., 1974. *Szczegółowa mapa geologiczna Sudetów 1:25 000. Arkusz Ziębice.* Wydawnictwa Geologiczne, Warszawa.

ZEH, A., BRAETZ, H., MILLAR, L.L. & WILLIAMS, I.S., 2001. Combined zircon SHRIMP and Sm-Nd isotope study of high grade paragneisses from the Mid-German Crystalline Rise; evidence for northern Gondwanan and Grenvillian provenance. *Journal of the Geological Society, London*, 158: 983–994.

ŻELAŹNIEWICZ, A., 2003. Postęp wiedzy o krystaliniku Sudetów w latach 1990—2003. [Development in the geology of the crystalline basement of the West Sudetes in 1990–2003]. In: Ciężkowski, W., Wojewoda, J. & Żelaźniewicz, A. (Eds), *Sudety Zachodnie od wendu do czwartorzędu*. WIND, Wrocław: 7–16.

ŻELAŹNIEWICZ, A., 2005. Przeszłość geologiczna. [Geological past]. In: J. Fabiszewski (Ed.), *Przyroda Dolnego Śląska*. Polska Akademia Nauk, Wrocław: 61–134.

ŻELAŹNIEWICZ, A. & ALEKSANDROWSKI, P., 2008. Regionalizacja tektoniczna Polski - Polska południowo-zachodnia. [Tectonic subdivision of Poland: southwestern Poland]. *Przegląd Geologiczny*, 56: 904–911.